20288

Project N° 199

RHEOLOGY AND PROCESSING OF COMPOSITE MATERIALS

by

L.A. Utracki
National Research Council of Canada
Industrial Materials Research Institute
750 Bel-Air, Montreal, Quebec H4C 2K3

CNRC N° 20288

RHEOLOGY AND PROCESSING OF COMPOSITE MATERIALS *

by

L.A. Utracki
National Research Council of Canada
Industrial Materials Research Institute
750, Bel-Air, Montreal, Quebec H4C 2K3

ABSTRACT

The increase in resin costs, paralleled by a reduction of choice of polymers available on the market, forces the plastics industry toward diversification via alloying and reinforcing. Thermoplastics and thermoset materials filled with inexpensive, mainly inorganic, particulates are an important class of engineering plastics. In this paper, the melt rheology and processing of the resins reinforced by particulates is reviewed. The flow behaviour of mica-filled polyethylene is discussed in greater detail.

* Based on the presentation at the mini-symposium "Composites-81" organized by and held at the Industrial Materials Research Institute, National Research Council of Canada; Montreal, December 8, 1981.

INTRODUCTION

The projected (1, 3) consumption of fillers and reinforcements by the North American plastics industry in 1990 is 6.7 millions metric tons, giving about 30% of market share to filled or reinforced plastics. There are two main reasons for using these systems: the performance and the economics. One cannot obtain the same high performance from the non-reinforced plastics as from the reinforced ones viz. automobile applications.

The consumption and cost of the most popular fillers are listed in Table 1. Prices of these materials are comparable to those of: polypropylene, PP, polyethylene, PE, polystyrene, PS, poly(vinyl chloride), PVC, poly(ethylene terephthalate), PET, and iononomer (1). This indicates that one should use fillers either with a more expensive resin or in order to achieve properties of one. Examples of cost calculations can be found in (5,6), e.g. in blending of polyester with $CaCO_3$ one can reduce the final material and production cost by 17%. It is clear that the cost saving obtained on a per volume basis is considerably less than that which is usually assumed. However, as the cost of feedstocks mounts, and as a result the price of the basic resins, increases, the use of fillers to become more and more attractive.

In order to process the composites, it is necessary to know the rheological behaviour of highly concentrated suspensions in

viscoelastic liquids, i.e. the systems which are most difficult to treat theoretically. In this presentation the following subjects will be discussed:

1. Interactions in filled polymer melts.
2. Rheology of Newtonian liquid suspensions.
3. Rheology of filled polymer melts.
4. Processing and rheology.

1. INTERACTIONS IN FILLED POLYMER MELTS

Interaction between the polymer matrix and particulate filler influences properties and ultimate usefulness of the finished product. Well dispersed and strongly bonded to the matrix fillers are desired. It has been shown (7) that for PS the melt consists of an assembly of interpenetrated random coils with dimensions comparable to those observed in theta solvents. The subjects was reviewed by Graessley and de Gennes (8).

The most widely used filler is $CaCO_3$, followed by talc, clay, silica, mica and glass (10). These represent a wide variety of shapes and particle sizes (Table 2). They all contain varying amounts of water adsorbed on the surface (11). Excepting the glass microspheres, they have relatively high density which may limit their usefulness. The nature of the filler-polymer interface in the melt have been seldom studied. In the case of low molecular weight liquids, the interfacial layer is only

several Angstroms (Å) thick, whereas that in high molecular weight fluids, it may reach several microns (20). The existence of this layer increases the effective apparent particle dimension and the concentration dependence of rheological functions. At higher concentration $\phi \doteq 0.15$ a macromolecule may participate in boundary layers of several particles leading to formation of a "secondary quasi-crosslinked network", which shows a time dependent rheological behaviour (21). In some cases, preferential adsorption of polymers, was observed (22). For minerals with preferential cleavage planes, the physical attachment of macromolecules to the others, less regular planes is more probable. In case of mica flakes such a preference increases the apparent aspect ratio and the filler effect on the rheological behaviour. In some cases the adsorbed macromolecule assumes a random coil configuration (22, 23).

In general, the filler-filler interactions are stronger than the matrix-filler ones (24, 25), and the particles tend to aggregate. The rheological properties of filled melts as well as the performance of the finished product are affected by the presence of aggregates. The best method to improve filler dispersion involves a treatment with surface active, or "sizing" agents (26). This reduces the filler-filler interactions, improve the filler-polymer bonding and may reduce the machine wear (27). For some polymer melts containing filler treated with a surface active agent the high shear viscosity may fall below that of the pure polymer (28,29).

2. RHEOLOGY OF NEWTONIAN LIQUID SUSPENSIONS

ZERO SHEAR PROPERTIES. The theoretical calculations for the zero shear viscosity of suspensions (30,31), lead to a power series equations for relative viscosity:

$$\eta_r = \eta/\eta_o = \Sigma\ a_i \phi^i \qquad (1)$$

where η and η_o are the zero shear viscosities of suspension and the suspending medium respectively, and ϕ is the volume fraction of suspended particles. The classical Einstein solution (32) for infinitely dilute hard sphere suspensions gives:

$a_o = 1$, $a_1 = 5/2$, $a_i\ (i > 2) = 0.$

Simha extended this treatment to rigid dumbells (33), ellipsoids of rotation and rigid rods (34):

$$a_1 = \frac{14}{15} + \frac{p^2}{5}\left(\frac{1}{3(\ln 2p - \lambda)} + \frac{1}{\ln 2p - \lambda + 1}\right) \qquad (2)$$

where: the aspect ratio $p = b_1/b_2$, with b_1 and b_2 major and minor axis of rotation respectively and λ a numerical constant. For ellipsoids of rotation $\lambda = 1.5$ and for rigid rods $\lambda = 1.8$.

As the concentration increases, so does the need for higher terms in Eq (1). However, even for moderate concentrations the theoretical difficulties are becoming very severe indeed; the values $a_2 = 2.5$ to 14.1 were reported (39). A rigorous

treatment of the cell model of hard spheres suspension resulted in an exceptionally useful relation (35):

$$\eta_r = 1 + 2.5\lambda\phi$$
$$\lambda = 4(1 - Y^7)/(4(1 + Y^{10}) - 25Y^3 (1 + Y^4) + 42Y^5) \qquad (3)$$
$$Y = (2(\phi_m/\phi)^{1/3} - 1)^{-1}$$

From the many $\eta_r = \eta_r(\phi)$ relations (36-38) the more successful are:

Krieger (39) $\eta_r = (1 - K\phi)^{-a_1/K}$ (4)

Fedors (40) $\eta_r = [1 + 1.25\phi/(\phi_m - \phi)]^2$ (5)

Quemada (41) $\eta_r = (1 - \tilde{\phi})^{-2}$; $\tilde{\phi} = \phi/\phi_m$ (6)

Gillespie (42) $\eta_r = (1 + \phi_{eff}/2)/(1 - \phi_{eff})^2$ (7)

$\phi_{eff} = \phi + k\phi^2$; $k = (1 - \phi_m)\phi^{-2}$.

Equation (4) written as:

$$\eta_r = (1 - \tilde{\phi})^{-2.5} \qquad (4a)$$

has been used (45) for suspensions containing particles of different shapes and sizes (ϕ_m was an experimental quantity determined by centrifugation).

On the basis of the free volume theory Utracki (44, 45) derived the following dependence:

$$\ln\eta_r = D_0 + D_1/(1 + D_2\phi) \qquad (8)$$

where D_i are parameters of the equation. For hard spheres suspensions $a_1 = 5/2$ and Eq (8) reduces to the Mooney (46) equation:

$$\ln\eta_r = 2.5\phi/(1 + D_2\phi) \qquad (9)$$

The relative merit of these relations can be evaluated by comparison, with the Thomas empirical dependence (42):

$$\eta_r = 1 + 2.5\phi + 10.05\phi^2 + 0.00273 \exp\{16.6\phi\} \quad (10)$$

(Note that $\eta_r \to 44{,}216$ for $\phi \to 1.0$!).

This equation was fitted to viscosity data of suspensions of uniform spherical particles obtained in sixteen different laboratories. The particle diameters varied from 0.099 to 435 μm. Both aqueous and non-aqueous systems were measured with $0.0 \leqslant \phi \leqslant 0.7$ (Fig. 1). By appropriate correction methods Thomas obtained a generalized dependence shown in Fig. 2. Equation (10) represents this generalized behaviour.

Setting $a_1 = 2.5$, the Eqs (3) - (9) were treated as single parameter dependencies, which value was calculated by equating:

$$\eta_r(i) = \eta_r(10)\big|_{\phi = 0.5}$$

(here the values in parenthesis refer to equation number: i = 3, ... 9). Next, for $\phi < 0.65$, the deviation:

$$\Delta\eta_r = 100\,[1-\eta_r(i)/\eta_r(10)] \quad (11)$$

was computed. The values of $\Delta\eta_r$ are shown in Fig. 3 and Table 4. The average, absolute deviation, $|\overline{\Delta\eta_r}|$, and the absolute maximum deviation, $|\Delta\eta_{r,max}|$ were also computed. The experimental data follow the theoretical Equations in the following order of accuracy: Eq (8), Eq (3), Eq (7) and Eq (6). In Fig. 4, the values calculated from the four best equations (points) are compared with the experimental curve (solid line) defined by Eq (10); Eqs (3) and (8) give the best fit.

A short note regarding Eqs (8) and (9). Fig. 5 illustrates the linearisation of the data (42). Relaxing the hard sphere requirement that $D_0D_2 = a_1 = 2.5$, one can use this type of plot to generalize any η_r vs. ϕ dependence, provided that the structure of liquid does not change within the range of the experimental conditions (44, 45). Earlier, Eq (3) has been successfully used (48) for hard sphere suspensions of PVC latexes and organosols. In these cases, ϕ_m was determined by centrifugation in a similar manner as in applications of Eqs (4a) and (5).

There are three aspects which may significantly complicate the analysis of η_r vs. ϕ dependence:

(i) polydispersity

(ii) particle shape

(iii) structure formation

Polydispersity. The overall relative viscosity of polydisperse suspension can be calculated as (49):

$$\eta_r = \Pi\, \eta_{r,i}\,(\Phi_i); \quad \Phi_i = V_i/\Sigma V_i \qquad (12)$$

(V_i is the volume of the i-th generation of spheres). It is customary to assign the subscript i = 0 to the liquid, i = 1 to either the smallest or the largest particles. Eq (12) shows that in order to operate at a minimum value for η_r at a constant-total-solids volume-fraction, ϕ_T, the distribution of the discrete particles should be: Φ_i = const.

Note that Φ_i is <u>not</u> defined in the customary way as a volume fraction of the total, but as a volume fraction of the volume up-to-and-including the i-th generation of spheres!

The viscosity of disperse spheres suspension has been expressed (50):

$$\eta_r = \Pi \exp \{ 2.5\ \phi_i/(1-k_i\phi_i) \} \qquad (13)$$

where ϕ_i's are the volume fractions of each generation of particles and k_i's depend on their diameter. Effect of bimodality of particle distribution is demonstrated in Fig. 6, (50). The minimum is a result of the increase of packing efficiency. A large body of literature on the subject has accumulated over the years. White and Walton (51) calculated that by selecting generations of spherical particles of proper relative diameters and composition one can increase ϕ_m from 0.7404 (single generation) to: 0.793 (binary), 0.810 (tertiary), 0.842 (quaternary), 0.851 (quinary) and 0.961 (hexagenary). Similar calculations (48) were qualitatively confirmed by blending specially prepared PVC latexes and subsequently measuring the η_r vs. ϕ dependence. The difference between the computation and experiments stems from the initial assumption of a perfect hexagonal packing with the coordination number of N = 12. The values of ϕ_m for mono and multimodal suspensions are listed in Table 5.

Shape. For non-spherical particles of ratio, p, the parameter $\phi_m = \phi_m(p)$. Fig. 7 illustrates the experimental dependence (59) where the ϕ_m^d refers to the dry packing; note that for p increasing from 1 to 50, ϕ_m^d decreases from 0.63 to 0.11. In particular, for p = 38 the dry packing $\phi_m^d = 0.14$. It is worth comparing this value with $\phi_m = 0.31$, calculated (40) from η of suspension of rods with p = 38. There are few possible reasons for the disagreement: the difference in polydispersity, reduced friction coefficient in suspension, non random orientation of rods in a flowing system and partial attrition on handling.

The above discussion on ϕ_m for rods is also applicable to discs (flakes); for random loading ϕ_m decreases with p (defined here as diameter to thickness ratio), ϕ_m^d for dry packing is lower than that calculated from solution, etc. As Mason (60) demonstrated, both discs and rods show a similar behaviour in flow - above certain critical concentration, ϕ_c, their rotation is impossible and a plug flow is obtained. In general $\phi_c < \phi_m^d < \phi_m$.

The second source of difference between the hard sphere and non-spherical particle suspensions is the value of the intrinsic viscosity, a_1. As demonstrated above, for spheres $a_1 = 5/2$ is well established theoretically and verified by experiments. For suspensions of ellipsoids and rods, a_1 calculated from

Eq (2) is shown in Table 6. The experimental results of a_1 vs. p for discs (61) are significantly lower (Fig. 8) than those predicted by Eq 2. Mason et al. (60) have demonstrated that a_1 is sensitive to orientation. For time averaged optimum orientation, one can write:

$$a_1 = p^3/[3(\ln 2p - \lambda)(p + 1)^2] \quad . \qquad (14)$$

The values of a_1 from Eq (14) form a lower limit for this parameter (see Table 6).

In all the above considerations a uniformely dispersed system was assumed. This assumption is rarely observed. Two types should be distinguished, (a) formed by the shear field (e.g. skin-core in long tube flows), and (b) formed by particle-particle interaction. The knowledge of structures (a) is important for proper interpretation of the flow phenomena (60, 63-65) or the shear coagulation (66). The knowledge of structures (b) is the key for utilisation of suspension rheology in processing (37). Since the effective volume fraction of dispersed particles increases with the increase of association, the η_r is strongly affected. In general η_r of this type of suspensions depends on the shear history.

SHEAR DEPENDENT PROPERTIES. Shearing the suspensions may lead to any of the following phenomena:

(i) yield stress

(ii) thixotropy or rheopexy

(iii) dilatancy or pseudoplasticity

or their combination. Since these phenomena are well described in the textbooks and reviews (38, 67-76), only a selective brief is given here.

Yield stress The data in Fig. (9) demonstrate the influence of processing on the rheological behaviour of mineral/water paste at constant concentration of solids (77). Milling time reduces both the yield stress, σ_y, and the apparent viscosity, η_a. The concentration dependence of σ_y (Fig. 10) follows the relation (77):

$$\sigma_y = K(\phi - \phi_o)^n \qquad (15)$$

where: ϕ_o is the highest volume fraction of particles at which $\sigma_y(\phi) = 0$; K and n are parameters.

The effect of yield stress on $\eta = \eta(\phi)$, is shown in Fig. 11. The master curve was obtained by simultaneous vertical and horizontal shifts of raw data by η_o and γ_o, respectively. The concentration dependence of these parameters is shown in Fig. 12 (78).

Both thixotropy and rheopexy are two aspects of the relatively slow change of structure upon shearing. Rheopexy usually occurs in concentrated dispersions over a narrow range of γ beyond which only thixotropy is observed. This leads to discontinuity in flow curves (79) as illustrated in Fig. 13. Examples of the rheopectic systems are given in Table 7. The

thixotropic behaviour may be described by the following relation (71):

$$\eta - \eta_{\infty}^{t} = (\eta_{o}^{t} - \eta_{\infty}^{t}) \exp \{ -t/\tau^{*} \}$$

where: η_{o}^{t} and η_{∞}^{t} refer to initial and final values of viscosity, t is the shearing time and τ^{*} the relaxation time, dependent on ϕ, temperature and $\dot{\gamma}$. Consequently the flow curve of a dispersion may be given in terms of either η_{o}^{t} or η_{∞}^{t}; in the first case, the flow curve refers to the initial structure, in the second to the continuously varying one, defined by the equilibrium morphology at a given $\dot{\gamma}$. The two flow curves are bounds for the apparent flow behaviour. Unfortunately when the data evaluation method is not mentioned, the results are useless for the reader.

Dilatancy and pseudoplasticity refer to (80) - an increase and a decrease, respectively of η with $\dot{\gamma}$ (80). Similar to rheopexy, the dilatancy is a less frequent. Two semi-empirical equations are used to describe the η vs. $\dot{\gamma}$ dependence for dispersions:

Cross (81): $\eta = \eta_{\infty} + (\eta_{o} - \eta_{\infty})/(1 + a\dot{\gamma}^{b})$ (17)

and Krieger (82): $\eta = \eta_{\infty} + (\eta_{o} - \eta_{\infty})/(1 + \tau/\tau_{a})$ (18)

In Eq (17) η_{o} and η_{∞} correspond to η at $\dot{\gamma} = 0$ and $\dot{\gamma} \to \infty$, and a and b are constants. Cross introduced "a" as a ratio of kinetic constants for link rupture and for the Brownian motion. In Fig. 14 the usefulness of Eq (17) is shown. The data

(83) refer to the water-in-oil emulsion flow in rotational and capillary rheometers.

The Eq (18) was derived from the consideration of the energy dissipation during doublet-formation of rotating spheres. Since

$$\eta\dot{\gamma} = \tau = \sigma_{12} \ , \tag{19}$$

τ is the true shear stress. The value of τ_a which linearizes the dependence is usually selected by trial and error. Both Eq (17), with four adjustable constants, and Eq (18), with three, can be directly applied only to systems without yield stress. One way to circumvent the problem is to incorporate the definition:

$$\sigma_{12} = \tau_o - \tau_y \tag{20}$$

(τ_o and τ_y are respectively apparent and yield shear stress) into Eqs (17) or (18). The other is to write a constitutive equation (84):

$$\tau = \tau_y + \tau_o + \eta_\infty\dot{\gamma} - \tau_o \exp\{-a\dot{\gamma}\} \tag{21}$$

(τ_y, τ_o, and a are parameters), valid for viscoelastic liquids, suspensions and emulsions.

For a limited range of $\dot{\gamma}$ the "power law" equation

$$\eta = K_1 \dot{\gamma}^{-m} \tag{22}$$

(where: $K_1 = \eta(\dot{\gamma}=1)$ and $0 < m < 1$ are constants) is most frequently used.

The first <u>normal stress difference</u> for diluted, hard sphere

suspensions, was expressed (90) as:

$$N_1 = \sigma \phi A (0.35 R_e^{0.5} - 2/3) \quad (23)$$

where σ is shear stress of the medium and Re is the particle shear Reynolds number. For non-spherical particles (91):

$$N_1 = k\sigma\phi\dot{\gamma}\varepsilon^2 D/[\dot{\gamma}^2 + 36D^2] \quad (24)$$

where k is a constant, ε is a measure of deviation from sphericity and D is the rotational Brownian diffusion coefficient. Both Eqs (23) and (24) are valid for suspensions in Newtonian liquids. The inertial effect of particles causes $N_1 < 0$ for low values of Re (viz. Eq 23). For small D, Eq (24) predicts that N_1 is independent of $\dot{\gamma}$ but varies with ϕ and ε^2.

The elongational viscosity, η_e, of suspensions strongly depends on the aspect ratio (92-94). As indicated in the last column of Table 9, the ratio η_e/η for rod-like suspensions is about 8-times larger than predicted by the Trouton rule and as observed for pure liquids. It was reported (93) that for glass fiber dispersed in polybutene (ρ = 0.89 g/cm^3; η = 283 (P), T = 23°C) η_e follows the theoretical dependence:

$$\eta_e/\eta = 3 + 4 \phi p^2/3 \ln(\pi/\phi) \quad (25)$$

for p varying from 282 to 1259 and $\phi \geq 0.01$.

3. RHEOLOGY OF FILLED POLYMER MELTS

The filled polymer melts constitute a particular class of

suspensions in which the suspending medium is a viscoelastic liquid. This means that in addition to all the effects discussed in the previous section one has to add those introduced by the viscoelastic and macromolecular character of the dispersing medium. Investigation of the entirety of this complex problem began only recently.

Most of the studies have been done at a single, high rate of shear in capillary rheometers (95-101). In the work (102) the authors used a wide range of $\dot{\gamma}$. They showed that talc filled PP at low $\dot{\gamma}$'s exhibited a strong yielding. Within the range of $\dot{\gamma} > 1$, the flow curves (Fig. 15) follow a single dependence. The σ_y was found to change with the filler surface treatment. Similar effects were reported (103) for PP/short glass fiber (Fig. 16), for glass bead filled styrene acrylonitrile (SAN) copolymer (104), and others. In the report on flow of PP filled with mica flakes (105), a steep increase of η with ϕ was observed (Fig. 17). This effect was particularly pronounced at low $\dot{\gamma}$'s, suggesting the yield.

During the past few years, filled polymers have become one of the most interesting systems to study (95-126). The notable publications on the subject are summarized in Table 9. The most investigated filled polymer is PP, then PE and PS. Most of the data are obtained in shear flow without measuring the N_1. η_e was determined for a few systems only. The data of Table 9 will be discussed under appropriate subtitles.

SHEAR VISCOSITY. Three phenomena should be mentioned: (i) σ_y - yield, (ii) $\eta = \eta(\phi)$ and (iii) the η-anomaly.

For the proper understanding of flow, yield effects should be eliminated by standard methods of data treatment, viz. Fig. 9. Dependencies such as shown in Figs. 15 to 17 indicate yielding. In filled polymer melts σ_y is a general phenomenon , favored by a decrease of particle size (127), an increase of ϕ and a decrease of $\dot{\gamma}$. Plot of σ_y vs. ϕ is shown in Fig. 18. Modification of particle surface, changes σ_y (114, 124, 126).

Concentration effects. In PP/talc for all compositions (15) the viscosity above a certain value of $\dot{\gamma}$ follows the same curve. Similar results were reported by Goel (119). For PP/FG (Fig. 16) analogous trend was noted (103), (121). However, for most other polymers, η increases with ϕ in the full range of investigated $\dot{\gamma}$ (105, 108-110, 114, 121, 124). An example of this behaviour is shown in Fig. 19 for PS and PE filled with FG (110).

An anomalous behaviour of η is illustrated in Fig. 20; addition of $\phi = 0.001$ of glass powder (2μm) reduced the shear viscosity of PS by 45%. Similar effect was observed for all 15 types of particulates dispersed in PS, PP and elastomers. The authors (113) suggested that the phenomenon originates in a reduced polymer segment density near the particulate surface.

MELT ELASTICITY. Four methods are used to measure: N_1 - the normal stress difference, B - the die swell parameter, ΔP_e - the Bagley correction and G' - the storage modulus.

The N_1 vs. σ_{12} plots provide a direct view into the different mechanisms of the flow of polymers filled with fibers (Fig. 21) and small particulates (Fig. 23). For σ_{12} = const, in the first case N_1 increases with ϕ (115, 125), in the second N_1, decreases (97, 115, 126). For glass beads of diameter 10 and 36 (μm) N_1 remains unchanged. Recently η and N_1 were measured in a steady state rotational mode for filled maleic anhydride polyester resin (128). When 20 to 30 (wt%) of high density PE (HDPE) particulates, d = 40(μm), were added, negative values of N_1 were obtained. It was observed that $-N_1$ is an increasing function of σ_{12}, independent of ϕ and shearing history. Reversing the shearing direction or changing the shearing time did not affect this unusual behaviour.

For neat polymers, the die swell measurements provide simple means of extending the normal stress data to the high range of $\dot{\gamma}$ (129). For filled systems, the correlation is seldom valid. In Fig. 23, B vs. $\dot{\gamma}$ is plotted (124) for FG filled polycarbonate melts; B decreases with ϕ in spite of N_1 increase in Fig. 21. A decrease of B with ϕ was reported for PS/FG (108), PE/TiO_2 (109), PP/Talc (119), PP/FG and polyamide 6,6/FG (121) systems. The reason for this decrease is most

likely due to the flattening of the velocity profile (plug flow) on increase of ϕ.

For PP/FG suspensions, the entrance pressure drop, ΔPe, was observed (120) to increase with ϕ, while at the same time B was observed to decrease (121). On the other hand, for PP/Talc (119) both ΔP_e and B were reported to decrease. A good, reliable set ot data of all four measures of melt elasticity: N_1, B, ΔP_e and G' is needed.

Dynamic testing has not been frequently used. Its superiority over the steady state flow method lies in the fact that the results are directly related to the material structure. One can easily visualize a situation where two samples cut from an extrudate, one in the machine the other in the transverse direction, will show different dynamic behaviour in the melt. This will not be observed in the steady state test.

In Figs. 24 and 25 the preliminary results of melt flow behaviour of HDPE/mica are shown (130). For comparison, the apparent steady state capillary viscosities are also included. It can be seen that an excellent agreement between η and η' for PE and for the sample containing 60% of mica was obtained, but the two sets of data for PE with 25% of mica did not superimpose. The reasons for selecting η' rather than η^* is a better superposition for the neat resin and an the absence

of σ_y for PE in the $\eta' \times \omega$ vs. ω plot (the dependence $\eta^* \times \omega$ vs. ω did indicate σ_y!). The correlation between the steady-state and dynamic rheological data have been previously discussed (131). The spread of data for 25 (wt %) dependence at low frequencies is due to time of shearing effects. The disagreement between η and η' probably originates in the time dependent structures, in a manner similar to the one observed in Fig. 13. The yield stress, σ_y (dynes/cm^2) calculated from these results obeys the relation (15) with $K = 1.2 \times 10^5$ and $n = 1.42$. The shear storage modulus, G' (dynes/cm^2), vs. ω is shown in Fig. 25. At low frequencies the melt elasticity is proportional to the mica content. However, at higher range of ω, the G' becomes independent of ϕ. The sample containing 25% of mica show an intermediate behaviour between that of the "lightly crosslinked rubber", for 60% filled PE and "highly branched polymer melt" behaviour of the neat PE (132). When the temperature is lowered the rubbery plateau is pushed toward a higher value and lower frequencies and the time-dependent anomaly of η' vs. ω observed for 25 (wt%) filled system becomes stronger (130).

ELONGATIONAL VISCOSITY, η_e, data for SAN filled with 50 μm-glass beads indicated (104) that for $\phi < 0.2$ the Trouton rule is obeyed while for the highest loading, $\phi = 0.363$, $\eta_e/\eta = 1.7 \pm 0.3$ was found. By contrast the systems containing sub-micron particles are known to exhibit yields stress in both the shear and elongational flow. The

ratio $\sigma_{11,Y}/\sigma_{12,Y}$ = 1.2 - 1.9 was reported (116). The filler surface treatment has a profound effect on the low deformation rate behaviour.

The elongational viscosities of fiber-filled polymer melts (108, 110, 115) can be summarized as follows: (i) because of the yield stress, $\sigma_{11,y}$, the Trouton ratio, $\eta_e/3\eta$, for low elongation rates, $\dot{\varepsilon}$, reaches a very large value (Fig. 26); at high $\dot{\varepsilon}$, by contrast with neat resins, the Trouton ratio for fiber filled systems falls below one; (ii) qualitatively the η vs $\dot{\varepsilon}$ dependence for fiber and sub-micron particles filled polymer melt is the same (viz. Figs 26, 27), (iii) whereas for suspensions of particles in Newtonian liquids η_e = const. over a wide range of $\dot{\varepsilon}$, for those in polymer melts η_e strongly depends on $\dot{\varepsilon}$ (yield).

Theoretical treatments for filled polymer melts have been reviewed and discussed in recent publications (127, 133-135). Using the cell theory, the shear viscosity of concentrated suspensions in power-law fluids with yield, was calculated (135). From constitutive equations the stress tensor for suspensions of hard spheres (127) and fibers (133) has been derived. The calculations (115) allowed for a good fit of η and η_e for particle reinforced PS (Fig. 27). The theory requires experimental determination of the yield stress. The thixotropicity can also be incorporated through the time

dependent yield function. The derivations for fiber filled polymer melts (133) provide a fair representation of η, η_e, transient viscosity, N_1 and the second normal stress difference, N_2. The rheological behaviour of both the particulate and fiber filled systems can be predicted (134) from the Lodge rubber-like model with a strain-dependent memory function. The time dependence can be calculated from the dynamic moduli in the linear viscoelastic region. The derivation allows the calculations of η, η^*, N_1, N_2 and the transient behaviour.

4. PROCESSING AND RHEOLOGY

The filled polymer melts are processed primarily by extrusion and injection molding. In commercial applications, it is desirable to mix different types of fillers/reinforcing agents in order to secure the best packing efficiency (59, 136). Using numerical methods (136), combinations of up to five different particulate and fibrous materials in the range of sizes from 0.5 to 250 μm may be optimized. These preparations can significantly reduce the raw material and processing costs , reduce wear of the equipment, ease the processing and improve the product. At high loadings and under the normal processing conditions, the key rheological property is the shear viscosity. With hindered rotation of particles a plug flow profile, zero normal stress differences, the time dependence of η and the

skin-core flow structure are to be expected. This means that for efficient processing of highly filled plastics, the compounding should be immediately followed by the processing step: extrusion, injection or transfer molding, spray-up, etc.

One of the basic problems in compounding is the reduction of aspect ratio of the fibers and flakes (114, 137). This can be partially prevented by: (i) surface coating of particulates, (ii) incorporating the particulates into polymeric liquids at the highest possible temperature, (iii) using twin-screw extruders, impinging mixers, or other types of equipment where mechanical or high shear breaking action is limited.

Extrusion is the basic plastic processing operation. For analysis of extrusion of filled materials, the standard methods of calculation (137-140) can be used. In a single screw extruder (108), the fiber breakage was found to be related to the screw speed and η. Most of the damage occured in the melting zone. The degree of damage increased with a decrease of temperature and increase of molecular weight. Using milder extrusion condition, i.e. low screw speed, low η, did reduce the damage but also the degree of dispersion. The presence of particulates has a beneficially effect on the melt fracture (140, 141); it increases the critical shear stress at which it occurs and decreases its intensity.

Injection molding requires higher $\dot{\gamma}$ and lower η than extrusion, what means lower loading of particulates and low viscosity of suspending liquids, i.e. the Reinforced Reactive Injection Molding (RRIM) is the ideal technology. Alternatives are transfer molding (142) or spray-up (136). Since the fiber orientation is desirable, the elongational and shear fields must be provided by a proper channel profile. It is important that the fiber concentration ($\phi < 0.4$) and the aspect ratio ($p \approx 25$) allow for the free rotation of particles.

The importance of mold geometry and temperature was demonstrated in a study of mold filling by PP, PP/glass blends and PP/FG (143). While the geometry determined the extent of fiber orientation, the temperature determined the thickness of the skin, i.e. the size of the core channel, and, in effect, the velocity profile in the mold. This work was continued (144) in simple end-gated molds where the effect of the processing conditions and rheology on fiber orientation was examined. It was found that high injection speeds favored a transverse alignement of fibers in the core while slow speeds favored the longitudinal orientation. Mouldings produced at high speeds had a glossy surface, while those at low speeds had a matt surface.

There is little information on the effects of rheology and processing on the flow orientaton of mica flakes in polymers (105, 145). During flow of concentrated suspensions in Newtonian

liquids through tubes (31) both fibers and discs aligned longitudinaly at the axis with the longest dimension in the direction of flow . In extrusion of mica filled PP (105), the opposite effect was observed; near the wall the flakes were parallel to the flow direction while near the center they were perpendicular. A similar structure was observed during injection molding (145), but there the core anisotropy was very low.

Machine wear during processing of filled materials is quite high (146, 147). Both corrosive and erosive wear were reported. The corrosive damage, (e.g. due to thermal decomposition of a sizing agent), causes an increase of barrel bore diameter, and a corresponding decrease of the screw diameter, both occuring at the front end. The abrasive (or erosive) wear is most severe in the melting zone of the extruder, where η and the pressure are the highest. The wear increases with filler hardness, particle size and aspect ratio and with the extent of agglomeration. It was reported that a modification the extrusion parameters increased the lifetime of the equipment by a factor of ten.

REFERENCES

1. L.A. Utracki and G.L. Bata, "Polymer Alloys" paper presented during CANPLAST, Montreal, Oct, 25-28, 1981; L.A. Utracki, paper N° 9 presented during "Polyblends-82", Montreal, April 28, 1982, Polymer Eng. Sci., in press

2. R.B. Seymour, Polym.-Plast. Technol. Eng., 7, 49 (1976)

3. D.G. Leis, J. Elastomer. Plast., 11, 301 (1979)

4. H.A. Arbit, Plast. Eng., 33 (1981), No. 5

5. T.H. Ferrigno in "Handbook of Fillers and Reinforcements for Plastics", J.V. Milewski and H.S. Katz, Eds, Van Nostrand Reinhold Co., New York, 1978

6. R.P. Braddicks Jr, and L.I.Nass in "Encyclopedia of PVC", L.I. Nass, Ed., Marcel Dekker Inc., New York, 1977 vol. 2

7. H.G. Kim, J. Appl. Polymer Sci., 22, 890 (1978)

8. W.W. Graessley, Adv. Polym. Sci., 16, 1, (1974); P.-G. de Gennes, "Scaling Concepts in Polymer Physics", Cornell U. Press, Ithaca, 1979

9. S.M. Aharoni, Macromolecules, 11, 680 (1980)

10. Anon., Plastics Engineering, May 1981, 33; R.B. Seymour, Polym. - Plast. Technol. Eng., 7, 49 (1976)

11. H. Burrel, A.C.S. Div. Org. Coatings and Plastics, Preprints, 35, 18 (1975)

12. J.Z. Keating, Plastics Compounding, 3 (4), 23 (1980)

13. G. Crove and P.E. Kummer, Plastics Compounding, 1 (3), 14 (1978)

14. J.A. Radosta, Plastics Compounding, 2 (5), 2 (1979)

15. M. Xanthos, Plastics Compounding, 2 (4), 19 (1979)

16. J.R. Copeland and O.W. Rush, Plastics Compounding, 1 (4), 26 (1978)

17. H.S. Katz and L. Ehrenreich, "Additions for Plastics", R.B. Seymour Ed., Academic Press, New York, 1977, vol. 2, 17

18. D.L. Muck and J.R. Ritter, Plastics Compounding, 2 (1), 12 (1979)

19. M.P. Wagner, "Additives for Plastics", R.B. Seymour Ed., Academic Press, New York, 1977, vol. 1, 9

20. L.A. Faitelson, Int. J. Polym. Mat., 8, 207 (1980)

21. L.A. Faitelson and E.E. Jakobson, Polymer Mech., 6, 898, (1977)

22. J. Klein, Nature, 288, 248 (1980)

23. F.R. Eirich, J. Coll. Interface Sci., 58, 423 (1977)

24. B.V. Deryagin, N.A. Krotova and V.P. Smilga, "Adhesion of Solids", Consultants Bureau, New York, 1978 282

25. E.P. Plueddemann, "Additives for Plastics", R.B. Seymour Ed., Academic Press, New York, 1977 vol. 1, 123

26. E.P. Plueddemann and G.L. Stark, "Additives for Plastics", R.B. Seymour Ed., Academic Press, New York, 1977 vol. 2, 49

27. S.J. Monte, G. Sugerman, Plastics Compounding, 1 (1), 56 (1978)

28. S.J. Monte and G. Sugarman, "Additives for Plastics", R.B. Seymour Ed., Academic Press, New York, 1977, vol. 2, 63

29. C.E. Chaffey, Proceedings 2nd World Congress of Chemical Engineering, Montreal, Oct. 1981, vol. V1, 301

30. H. L. Frisch and R. Simha in "Rheology" F. R. Eirich, Ed., Academic Press, New York 1956, Ch 14.

31. H. Brenner, Progr. Heat Mass Transfer, 5, 89 (1972)

32. A. Einstein, Ann. Physik, 17, 549(1905); 19, 289, (1906); 34, 591 (1911)

33. R. Simha, J. Res. NBS, 42, 409 (1949); J. Colloid Sci., 5, 386 (1950)

34a. R. Simha, J. Phys. Chem., 44, 25 (1960); J. Chem. Phys., 13, 188 (1945)

34b. J.W. Mehl, J.L. Oncley and R. Simha, Science, 92, 132 (1940)

35. R Simha, J. Appl. Phys., 23, 1020 (1952)

36. Ir. R. Rutgers, Rheolog. Acta, 2, 305 (1962)

37. T. L. Smith, J. Paint Technol., 44, 71 (1972)

38. D. J. Jeffrey and A. Acrivos, AIChE J., 22, 417 (1976)

39. I.M. Krieger in "Surface and Coatings Related to Paper and Wood", R. Marchessault and C. Skaar, Eds., 1967.

40. R. F. Fedors, Polymer, 16, 305 (1975)

41. D. Quemada, Rheolog. Acta, 16, 82 (1977)

42. T. Gillespie, Proceed.50th Intl. Conf. Colloid Interface Sci., 4, 465 (1976)

43. R. F. Landel, B. G. Moser and A. J. Bauman, Proceedings 4th Intl. Congress Rheology, USA, 1963

44 L. A. Utracki, J. Macromol Sci. Phys., B18, 725 (1980)

45. L. A. Utracki and R. Simha, J. Rheolog., 25, 329 (1981)

46. M. Mooney, J. Colloid Sci., 6, 162 (1951)

47. D. G. Thomas, J. Colloid Sci., 20, 267 (1965)

48. L. A. Utracki, Gulf Oil Canada internal reports, 1970, 1971

49. R. J. Farris, Trans. Soc. Rheology, 12, 281 (1968)

50. C. Parkinson, S. Matsumoto and P. Sherman, J. Colloid Interface Sci., 33, 150 (1970)

51. H.E. White and S.F. Watson, J. Amer. Ceram. Soc., 20, 155 (1937)

52. A.E.R. Westman and H.R. Hugill, J. Amer. Ceram. Soc., 13, 767 (1930)

53. M.M. Bernarie, Br. J. Appl. Phys., 12, 514 (1961)

54. R.K. Mc Geary, J. Amer. Ceram. Soc., 44, 513 (1961)

55. S. Yerazunis, J.W. Bratlett and A.H. Nissan, Nature, 195, 33 (1962)

56. R. Farley and F.H.H. Valentin, Preprint Symp. Powder Flow, Storage, Bradford, Sept. 1967

57. J.L. Finney, Proc. Roy. Soc. London, A319, 479 (1970)

58. J. Ritter, Appl. Polymer Symp. No 15, 239 (1971)

59. J.V. Milewski, 29 Ann. Techn. Conf., SPI, Reinforced Plastics Div., Febr. 1974; Ind. Eng. Prod. Res. Dev., 17, 363 (1978)

60. H.L. Goldsmith and S.G. Mason, in "Rheology", F.R. Eirich, Ed., Vol. 4, Academic Press, New York, 1967

61. P.S. Lingard and R.L. Whitmore, Chemeca, 11 (1970)

62. L. Nicodemo and L. Nicolais, Polymer, 15, 589 (1974)

63. A. Brandt and G. Bugliarello, Trans. Soc. Rheology, 10, 229 (1966)

64. A. Okagawa and S.G. Mason, Can. J. Chem., 53, 2689 (1975)

65. J.B. Harris and J.F.T. Pittman, Trans. Inst. Chem. Eng., 54, 73 (1976)

66. L.A. Utracki, J. Colloid Interface Sci., 42, 185 (1973)

67. A. van Buzagh, "Colloid Systems", Techn. Press, London, 1937

68. R.J. Hartman, "Colloid Chemistry", Houghton Mifflin Co., Boston, 1939

69. E.K. Rideal, Ed. "Colloid Science", Chem. Publ. Co., N.Y. 1947

70. H. Green, "Industrial Rheology and Rheological Structures", J. Wiley, London, 1949

71. J.J. Hermans, Ed., "Flow Properties of Dispersed Systems", Intersci. Publ., N.Y. 1953

C.C. Mill, Ed., "Rheology of Dispersed Systems", Pergamon Press, London, 1959

72. J.R. Van Wazer et al., "Viscosity and Flow Measurements", Intersci. Publ., N.Y. 1963

73. P. Sherman, Ed., "Rheology of Emulsions", Pergamon Press, Oxford, 1963

74. P. Sherman, Ed., "Emulsion Science", Academic Press, London, 1968

75. W.A. Bauer and E.A. Collins, "Thixotropy and Dilatancy" in "Rheology" Vol. 4, E.R. Eirich, Ed., Academic Press, New York, 1968

76. J. Raczkowski, "Reologia cieczy wiertniczych" (Rheology of Mining Fluids), W.G., Warszawa, 1975

77. L.A. Utracki, unpublished.

78. L. Nicodemo and L. Nicolais, J. Appl. Polymer Sci., 18, 2809 (1974)

79. R.L Hoffman, Trans. Soc. Rheology, 16, 155 (1972); J. Colloid Interface Sci., 46, 491 (1979)

80. M. Reiner and G.W. Scott Blair, in "Rheology" Vol. 4, E.R. Eirich, Ed., Academic Press, New York, 1967

81. M.M. Cross, J. Colloid Sci., 20, 417 (1965), ibid. 33, 30 (1970), ibid. 44, 175 (1973)

82. I.M. Krieger and T.J. Dougherty, Trans. Soc. Rheolog., 3, 137 (1959)

83. L.A. Utracki and M.R. Kamal, Polymer Eng. Sci., 22, 96 (1982)

84. J.T. Fisher and B.B. Sheth, Aerosol Age, 1973 (2), 28-31, 56, ibid. 1973 (3), 22-25

85. T. Gillepsie, J. Colloid Interface Sci., 22, 554 (1966)

86. R.J. Morgan, Trans. Soc. Rheology, 12, 511 (1968)

87. Yu.E. Pivinskii, Kolloid Zhurn., 35, 286 (1973)

88. J. Barbee, Trans. Soc. Rheology, 17, 413 (1973)

89. I.M. Krieger, Adv. Colloid Interface Sci., 3, 111 (1972)

90. G.J. Lin, J.H. Perry and W.R. Schowalter, J. Fluid Mech., 44, 1 (1970)

91. E.J. Hinch and L.G. Leal, J. Fluid Mech., 52, 683 (1972)

92. C.B. Weinberger and J.D. Goddard, Intern. J. Multiphase Flow, 1, 465 (1974)

93. J. Mewis and A.B. Metzner, J. Fluid Mech., 62, 593 (1979)

94. T.E. Kizior and F.A. Seyer, Trans. Soc. Rheology, 18, 271 (1974)

95. C.C. McCabe and H.W. Mueller, Trans. Soc. Rheology, 5, 329 (1961)

96. J.R. Hopper, Rubber Chem. Technol., 43, 405 (1970)

97. C.D. Han, J. Appl. Polym. Sci., 18, 821 (1974)

98. J.L. White and J.W. Crowder, J. Appl.Polym. Sci., 18, 1013 (1974)

99. N. Nakajima and E.A. Collins, Rubber Chem. Technol., 48, 615 (1975)

100. Y. Oyanagi and Y. Yamaguchi, J. Soc. Rheol. Japan, 3, 64 (1975)

101. C.D. Han, C. Sandford and H.J. Yoo, Polym. Eng. Sci., 18, 851 (1978)

102. F.M. Chapman and T.S. Lee, SPE, ANTEC, 15, 293 (1969)

103. J.-M. Charier and J.M. Rieger, Fibre Sci. Technolog., 7, 161 (1979)

104. F. Nazem and C.T. Hill, Trans. Soc. Rheology, 18, 87 (1974)

105. K. Okuno and R.T. Woodhams, Polymer Eng. Sci., 15, 308 (1975)

106. N. Mills, J. Appl. Polym. Sci., 15, 2791 (1971)

107. V.K. Kamlev and A.M. Braginskii, Intl. Chem. Eng., 12, 43 (1972)

108. J.L. White and Y. Oyanagi, SPE-ANTEC, 35, 290 (1977)

109. J.L. White, Rubber Chem. Techn., 50, 163 (1977)

110. Yu Chan, J.L. White and Y. Oyanagi, J. Rheology, 22, 507 (1978)

111. T. Kataoka, T. Kitano and T. Nishimura, Rheol. Acta, 17, 626 (1978)

112. E.A. Moscal, SPE-RATEC, Oakbrook, Ill., Oct. 2 to 4, 1979, paper No. H-1

113. V.V. Prokopenko, O.K. Titova, N.S. Fesik, Yu.M. Malinskii and N.F. Bakeyev, Vysokomol. Soed., A 19, 95 (1977)

114. L. Czarnecki and J.L. White, J. Appl. Polymer Sci., 25, 1217 (1980)

115. J.L. White, L. Czarnecki and H. Tanaka, Rubber Chem Techn., 53, 823 (1980)

116. H. Tanaka and J.L. White, Polymer Eng. Sci., 20, 949 (1980)

117. D.P. Thomas and R.S. Hagen, SPI Annual Meeting, (1966)

118. C.D. Han, J. Appl. Polymer Sci., 18, 821 (1974)

119. D.C. Goel, Polymer Eng. Sci., 20, 198 (1980)

120. R.J. Crowson, M.J. Folkes and P.F. Bright, Polymer Eng. Sci., 20, 925 (1980)

121. R.J. Crowson and M.J. Folkes, Polymer Eng. Sci., 20, 934 (1980)

122. J. Kubat and H.-E. Stromwall, Plastics Rubber Process., 5, 45 (1980)

123. P. Bataille and T.V. Bui, Polymer Composites, 2, 8 (1981)

124. B.A. Knutsson, J.L. White and K.B. Abbas, "Rheology" Vol. 3, 83 (1980), VIII Intl. Congr. Rheology, G. Astarita, G. Marrrucci and L. Nicolais, Eds. Plenum Press, New York 1980

125. A.K. Bagchi and K.K. Sirkar, J. Appl. Polymer Sci., 23, 1653 (1979)

126. K. Iwakura and T. Fujimura, J. Appl. Polymer Sci., 24, 975 (1979)

127. J.L. White, Proceed. 2nd World Congress Chem. Eng., Montreal, October 4-9, 1981, Vol. VI, 296

128. C.D. Han and K.W. Lem, Paper EII presented during 53rd annual meeting Soc. Rheology, Louisville, Oct. 11-15, 1981

129. L.A. Utracki, Z. Bakerdjian and M.R. Kamal, J. Appl. Polymer Sci., 19, 481 (1975)

130. B. Fisa and L.A. Utracki, paper presented at the 65 CIC Conference, Toronto, May 30 - June 3, 1982; to be published in Polymer Eng. Sci.

131. W.P. Cox and E.H. Merz, J. Appl. Polymer Sci., 28, 619 (1958); J.S. Wang, J.R. Knox and R.S. Porter, J. Polymer Sci. Polym. Phys. Ed., 16, 1709 (1978); R.M. Schulken, R.H. Cox and L.A. Minnick, J. Appl. Polymer Sci., 25, 1341 (1980)

132. J.D. Ferry, "Viscoelastic Properties of Polymers", J. Wiley and Sons, New York, 1970

133. S.M. Dinh and R.C. Armstrong, Proceed. 2nd World Congress Chem. Eng., Montreal, Oct. 4-9, 1981

134. R. Pisipati and D.G. Baird, paper presented at the 53rd annual meeting Soc. Rheology, Louisville, Oct. 11-15, 1981

135. H. Tanaka and J.L. White, J. Non-Newt. Fluid Mech., 7, 333 (1980)

136. viz. J.V. Milewski, Plastics Compounding, 26, May/June 1978

137. J.M. Lunt and J.B. Shortall, Plast. Rubb. Process, June 1980, 37

138. A.A. Veshchev and N.P. Shanin, Sov. Rubb. Techn., 31, 18 (1972)

139. W. Hsu, J.S. Shen, C.Y. Hsieh and H.Ito, Intl. J. Polymer Mat., 5, 303 (1977)

140. D.W. Clegg, A.A. Collyer and N.C. Griffin, Polymer, 21, 1360 (1980)

141. H.P. Schreiber, J. Polymer Sci., Polymer Letters, 7, 851 (1969)

142. L.A. Goettler, 25th Ann. Conf. Reinf. Plast. Comp. SPE, paper 14A, 1970; Proceed. 6-PAP Symp. Comp. Mater. Eng. Des., St-Louis, May 11-12, 1972, 480

143. L.R. Schmidt, Adv. Chem. Ser. , 142, 415 (1974)

144. P.F. Bright, R.J. Crowson and M.J. Folkes, J. Mater. Sci., 13, 2497 (1978)

145. R.G. Nelb, C.J. MacGregor and R.A. Parker, Automot. Eng., March 1979, 50

146. B.A. Olmsted, SPE J., 26, 42 (1970)

147. D.Braun and P. Volz, Mech. Mies. Nauk. Tech., 53, 155 (1980)

Table 1. Filler consumption in 1979 (4).

Material	Usage (1000 tons)	Costs (US cents) per pound	per cub. inch
Calcium carbonate	1388	4 to 18.50	0.4 to 1.8
Talc	163	1.50 to 4.50	0.2 to 0.5
Clays	131	1.25 to 19	0.1 to 1.8
Silicas	50	20 to 32.50	1.9 to 3.0
Mica	14	6.75 to 18	0.7 to 1.9
Glass	12	26	2.3
Miscellanous	176		
Total	1934		

Table 2. Particle dimensions and shapes of typical fillers.

Filler	Density ρ (g/ml)	Hardness (Mohs)	Typical Particle Size (μm)	Particle shape	Refs
Alumina trihydrate (ATH)	2.4	2.5	2-20	irregular	12
Calcium carbonate	2.71	3	1-10	irregular	13
Talc	2.4	1	3-8	platelets, aspect ratio 5.1 to 10.1	14
Mica	2.83	2-3	thickness t > 1	thin platelets 10-80 (μm) size	15
Wollastonite	2.98	4.5	10-30 aspect ratio 3.1 to 20.1	acicular	16
Glass fiber	2.55	6	diameter 9 to 18	fiber	17
Glass beads	2.5	6	30	spherical	17
Glass microspheres	0.1-0.5		70	spherical	18
Silica	2.6	7	natural 2-12 synthetic 0.01-0.1	complex spherical	19

Table 3. Effect of filler treatment (26).

(Percent of viscosity change of filled mineral oil; Brookfield viscometer; $\dot{\gamma} = 1$).

0.4% additive based on filler	Suspensions Containing: 27% Silica	50% $Al(OH_3)$	50% $CaCO_3$
Control η (cp)	25,000	22,100	40,500
	ORGANIC ADDITIVES		
Undecenoic acid	-35	-93	-93
1-Decanol	-38	-48	-49
1-methoxy-2 propanol	-40	-52	-53
Hexylamine	-68	-56	-54
$Ti(OBu)_4$	-69	-95	-95
$Al(OBu)_3$	-62	-85	-69
	SILANE ADDITIVES		
Z-6030	-52	-86	-47
Z-6030W decanol	-56	-85	-70
Z-6030 - $Ti(OBu)_4$	-64	-92	-91
Z-6030 - $Al(OBu)_3$	-64	-88	-80
Z-6032z (S) (Dow PM)	-43	-72	-70
Z-6032 (Dow PM)	-49	-84	-75

Table 4 - The deviation, $\Delta\eta_r$, computed from Eq (11) for Eqs (3) - (8).

ϕ	$\Delta\eta_r$ (%)						
	Eq (3)	Eq (4)	Eq (5)	Eq (6)	Eq (7)	Eq (4a)	Eq (8)
0.00	0.	0	0	0	0	0	0
0.05	-1.683	-1.459	3.165	1.025	-1.257	2.793	-1.299
0.10	-3.991	-3.652	6.340	1.314	-2.872	4.863	-2.991
0.15	-5.590	-5.691	8.985	1.733	-3.998	7.044	-4.162
0.20	-5.559	-6.917	12.217	2.967	-4.000	10.009	-4.108
0.25	-3.551	-7.154	16.123	5.175	-2.725	13.864	-2.600
0.30	0.123	-6.721	19.973	7.859	-0.576	17.912	0.028
0.35	4.207	-6.420	21.966	9.693	1.366	20.377	2.706
0.40	6.465	-7.044	19.584	8.845	1.644	18.681	3.779
0.45	4.887	-7.511	11.490	4.623	0.034	11.258	2.273
0.50	0.005	-0.006	0.004	0.000	-0.000	0.001	0.001
0.55	-4.233	64.602	-8.842	4.063	14.675	-9.775	2.709
0.60	-1.224		-5.161	49.299	117.313	-10.704	22.341
0.65	22.681		49.174	842.856		14.267	274.148
Parameter:	ϕ_m = 0.7864	K = 1.6896	ϕ_m = 0.71055	ϕ_m = 0.66844	ϕ_m = 0.65021	ϕ_m = 0.74848	D_2 = 1.09312
$\lvert\overline{\Delta\eta}\rvert$	3.66	10.651	11.74	4.30	3.01	10.60	2.42
$\pm\ \sigma$	2.17	18.07	7.09	3.31	4.12	6.67	1.45
$\lvert\Delta\eta_{r,max}\rvert$	6.465	64.602	21.996	9.693	14.675	17.912	4.162

Table 5: Packing efficiency (51) - (58).

N°	Suspension of		ϕ_m
I	Spheres: monomodal	N^c	
	hexagonal	12	0.7404
	face centered cubic	12	0.7404
	body centered cubic	8	0.60
	cubic	6	0.52
	random (theoretical)	-	0.637
	random (experimental)	-	0.60 - 0.64
II	Spheres: bimodal		
	random,		
	$d_2/d_1 = 1$		0.636
	$d_2/d_1 = 3.8$		0.684
	$d_2/d_1 = 47$		0.814
	$d_2/d_1 = \infty$		0.868
III	Spheres: quatromodal		
	theory		0.98
	experiment		0.81
IV	Crushed glass rod particles		
	monomodal		0.476-0.500
	bimodal		0.566
V	Precipitated $CaCO_3$		0.36-0.50
VI	Aluminium powder		0.25-0.32

Table 6. Intrinsic viscosity of non-spherical particles.

p	a_1 (ellipsoids)		a_1 (rods)	
	Eq(2)	Eq(14)	Eq(2)	Eq(14)
5	(4.71)	1.442	(5.81)	2.303
10	(8.04)	1.842	(13.63)	2.304
20	38.203	2.763	42.743	3.201
40	120.375	4.403	131.579	4.915

Note: The values in parentheses are taken from (34b).

Table 7. Rheopectic systems.

No	Medium	Dispersed phase			References
		Particles of	ϕ	d(μm)	
1.	Plasticizers	PVC	0.26-0.55	0.05-0.7	85
2.	Water	Fe_2O_3	0.41-0	0.1 -5.0	77, 86
3.	Water	SiO_2	0.62-0.87	2.5 -25	87
4.	Plasma	Blood cells	0.45-0.48	4.0	88
5.	Water	PS latex	0.4-0.5	0.1-0.6	89

Table 8. η and η_e for suspension of glass fibers, $\phi = 0.013$, $p = 57$ (92).

No	Fluid	η(P)	η_e(P)	η_e/η
I	Newtonian liquids			
	Silicone oil	1000	3000	3
	Indopol, (polybutene oil)	205	615	3
II	Suspensions			
	in silicone oil	1150	29,000	25
	in Indopol	235	5,400	23

Table 9. Summary of melt rheological investigation of the composites.

N°	Polymer/filler	Particulates			Measurements					Ref.
		d (μm)	p	ϕ_{max}	$\dot{\gamma}_{min}$	η	N_1	σ_y	η_e	
I	POLYETHYLENE (PE)									
1.	Fiber glass (FG)	10	400	0.20	30	η	-	Y	-	106
2.	Chalk, limestone	15	-	0.45	10	η	-	-	-	107
3.	FG	--	-	0.19	0.002	η	-	?	Y	108
4.	TiO_2	-	-	0.36	0.008	η	B	Y	-	109
5.	FG	12.7	157	0.19	0.005	η	Y	Y	Y	110
6.	Glass Balloons (GB)	53	-	0.653	10^{-9}	η	-	Y	-	111
	Carbon Fibers (CF)	10	60	0.044	10^{-3}	η	-	N	-	111
7.	FG	725	35	0.09	100	η	-	N	-	112
8.	Mica			0.33	0.01	η η*	G'		-	this work

Table 9. (cont.)

N°	Polymer/filler	Particulates d	Particulates p	ϕ_{max}	$\dot{\gamma}_{min}$	Measurements η	Measurements N_1	Measurements σ_Y	Measurements η_e	Ref.
II	POLYSTYRENE (PS)									
1.	Glass powders Kaolin, Alumina..	0.02 to 180	0 to 20	0.08	0.8	η	-	Anomaly -		113
2.	FG	12.7	15	0.22	0.01	η	Y	N		114
	Aramid (Kevlar)	12.2	60	0.18	0.01	η	Y	N		114
	Cellulose	12	100	0.20	0.01	η	Y	N		114
3.	$CaCO_3$	0.5	-	0.2	0.01	η	Y	Y	Y	115
	Carbon black (CB)	0.045	-	0.2	0.01	η	Y	Y	Y	115
	TiO_2	0.18	-	0.2	0.01	η	Y	Y	Y	115
	Franklin Fiber	1.5-2	100	0.2	0.01	η	Y	Y	-	115
	Mica	5	25-50	0.2	0.01	η	Y	N	-	115
	Glass Beads	10	-	0.2	0.01	η	Y	N	-	115
4.	Glass Beads	36	-	0.369	10^{-3}	η	-	Y	-	111
5.	FG	12.7	157	0.2	10^{-3}	η	Y	N	Y	110
6.	$CaCO_3$	0.5	-			η	Y	Y	Y	116
	CB	0.045	-			η	Y	Y	Y	116

Table 9. (cont.)

N°	Polymer/filler	Particulates			Measurements					Ref.
		d	P	ϕ_{max}	$\dot{\gamma}_{min}$	η	N_1	σ_Y	η_e	
III	POLYPROPYLENE (PP)									
1.	Talc	10	-	0.2	10^{-3}	η	-	Y	-	102
	Glass Beads	44	-	0.2	10^{-3}	η	-	Y	-	102
2.	FG			0.2	0.38	η	-	N	-	117
3.	FG			0.194	0.1	η	-	?	-	103
4.	Mica	6.7	65	0.15	2.5	η	-	?	-	105
5.	$CaCO_3$						-		-	118
6.	Fluoroplast	1.0	?	0.01		η	-	Anomaly	-	113
7.	FG	725	35	0.09	100	η	-	N	-	112
8.	Talc	30	-	0.2	150	η	B, Bagley	N	-	119
9.	FG (B)	10	50	0.07	3	η	B, Bagley	N	-	120-121
	FG (C)	10	30	0.11	1	η	B	N	-	121
	FG (D)	10	500	0.09	1	η	B	N	-	121
	FG (E)	10	1000	0.09	1	η	B	N	-	121
	FG (F)	10	2000	0.09	1	η	B	N	-	121
10.	FG	10	300	0.11	10	η	-	N	-	122
11.	Mica			0.17	0.5	η	-	N	-	29
	$CaCO_3$			0.22	0.2	η	-	N	-	29

Table 9. (cont.)

N°	Polymer/filler	Particulates			Measurements					Ref.
		d	p	ϕ_{max}	$\dot{\gamma}_{min}$	η	N_1	σ_Y	η_e	
IV	POLYVINYL CHLORIDE (PVC)									
1.	$CaCO_3$	?	-	0.21	?	η	-	-	-	123
	Mica	6	62.4	0.21	?	η	-	-	-	123
V	POLYCARBONATE (PC)									
	FG	12	?	0.24	0.1	η	Y, B	Y	-	124
VI	POLYAMIDE 6 (PA-6)									
	FG	10	300	0.11	10	η	-	-	-	122
VII	POLYAMIDE 6,6 (PA-6,6)									
	FG	10	30	0.19	10	η	B	N	-	121
VIII	RUBBERS									
	A. SBR / CB	0.045	-				-	?	-	98
	B. NR / CB	0.17	-	0.5	4.5	η	B	?	-	125
IX	SURLYN IONOMER									
	Perlite	5.5	-	0.15	0.04	η	Y	Y	-	126
X	POLY(STYRENE-CO-ACRYLONITRILE) (SAN)									
	Glass Beads					η	-	N	-	102

Notes: Significance of the symbols used in Table 9: η, η* - steady state and dynamic viscosities respectively; " - " = not measured, Y = yes; N = no; B, G', and Bagley - methods of measurements of the normal stress via: die swell, storage modulus, and from Bagley correction, respectively; "Anomaly" - rapid decrease of with addition of small volume of particulates: ? - uncertain.

LEGEND FOR FIGURES

Fig. 1 Relative viscosity of hard spheres suspensions, η_r vs. volume fraction, ϕ. Raw data (47).

Fig. 2 Corrected η_r vs. ϕ of hard spheres (47). The solid line represents Eq (10).

Fig. 3 Percent of difference between the theoretically predicted and empirically determined η_r as a function of ϕ. Numbers refer to the equations as listed in the text.

Fig. 4 η_r vs. ϕ as given by the empirical Eq (10) and predicted theoretically by Eqs (3), (6), (7) and (9). The parameters of these equations are listed in Table 4.

Fig. 5 Linearisation of η_r vs. ϕ dependence according to Eq (9). Points: experimental data.

Fig. 6 Effect of composition of suspension in bimodal size distribution of η_r, ϕ = 0.117; squares = 0.6, triangles = 1, circles = 4 (μm) diameter particles added to 0.1 (μm) ones (50).

Fig. 7 Effect of rod aspect ratio, p, on maximum dry packing volume fraction (59).

Fig. 8 Intrinsic viscosity, a_1 vs. aspect ratio, p, for discs (circles), red cells (triangle) (61) and glass fibers (square) (61).

Fig. 9 Yield stress determination for mineral suspension in water at ϕ = 0.71 and T = 25°C. Numbers refer to milling time in min. just prior to the capillary flow measurements (77).

Fig. 10 Yield stress vs. ϕ for mineral suspensions (77). The curve represents Eq (15).

Fig. 11 Reduced viscosity vs. reduced rate of shear for suspensions of glass beads in 4% poly(isobutene) solutions in decalin ϕ = 0.0, 0.1, 0.2, 0.3 and 0.4, T = 27°C (78).

Fig. 12 The reducing parameters η_o and $\dot{\gamma}_o$ of the data shown in Fig. 11 vs. ϕ (78).

Fig. 13 Flow curves of PVC (particle diameter 1.25 μm) in di-octyl phthalate at 25°C for ϕ = 0.47, 0.49, 0.51, 0.55 and 0.57 (79).

Fig. 14 Flow curve for water-oil emulsion at 25°C. Data from rotational and capillary rheometers; the curve represents the Cross Eq (17) with the parameters indicated (83).

Fig. 15 Flow curves for PP at 200°C filled with 0.0, 10, 20, 30 and 40 (wt %) of talc (102).

Fig. 16 Flow curves for PP at 205°C filled with ϕ = 0.0, 0.8 and 0.19 of glass fibers (103).

Fig. 17 Relative viscosity at constant $\dot{\gamma}$ vs. ϕ for PP/mica (three upper curves), for PP/$CaCO_3$ ($\dot{\gamma}$ = 10) and as calculated from Eq (2) i.e. at $\dot{\gamma}$ = 0 (105) (see text).

Fig. 18 Apparent yield stress σ_y vs. ϕ for PS filled with glass beads and balloons; line - Eq (15) with ϕ_o = 0, points (111).

Fig. 19 Flow curves for PS (upper diagram) and high density PE (lower diagram) at 180°C filled with 0, 20 and 40 (wt %) of glass fibers (110). WR and ICR indicate the Weissenberg Rheogoniometer and Instron Capillary Rheometer, respectively.

Fig. 20 Melt viscosity of PS at 188°C and at shear stress $\sigma_{12} = 2 \times 10^5$ (dynes/cm^2) vs. ϕ of glass powder (113), Δ = 45% indicate the maximum depression of η.

Fig. 21 N_1 vs. σ_{12} for polycarbonate at 250°C filled with 0.0, 10, 30 and 40 (wt %) of glass fibers (124).

Fig. 22 N_1 vs. σ_{12} for PS at 180°C filled with ϕ = 0.20 of, from the top, PS, glass beads, Franklin fibers, TiO_2, $CaCO_3$, carbon black and mica (115).

Fig. 23 Die swell ratio B vs. wall shear rate for polycarbonate, PC, at 290°C filled with 0, 10, 30 and 40 (wt %) of glass fibers (124).

Fig. 24 Flow curves for high density PE at 210°C filled with 0, 25 and 60 (wt %) of mica. Data from capillary (η_a) and dynamic (η') tests (130).

Fig. 25 Shear storage modulus, G', vs. frequency for high density PE at 210°C and strain 35%, filled with 0, 25 and 60 (wt %) of mica.

Fig. 26 Trouton ratio vs. deformation rate for PS at 180°C filled with 0, 20 and 40 (wt %) of glass fibers (108).

Fig. 27 Elongational viscosity vs. elongation rate for PS at 180°C filled with, from the top: $CaCO_3$, carbon black, TiO_2 and for pure PS. The curves are theoretical (115).

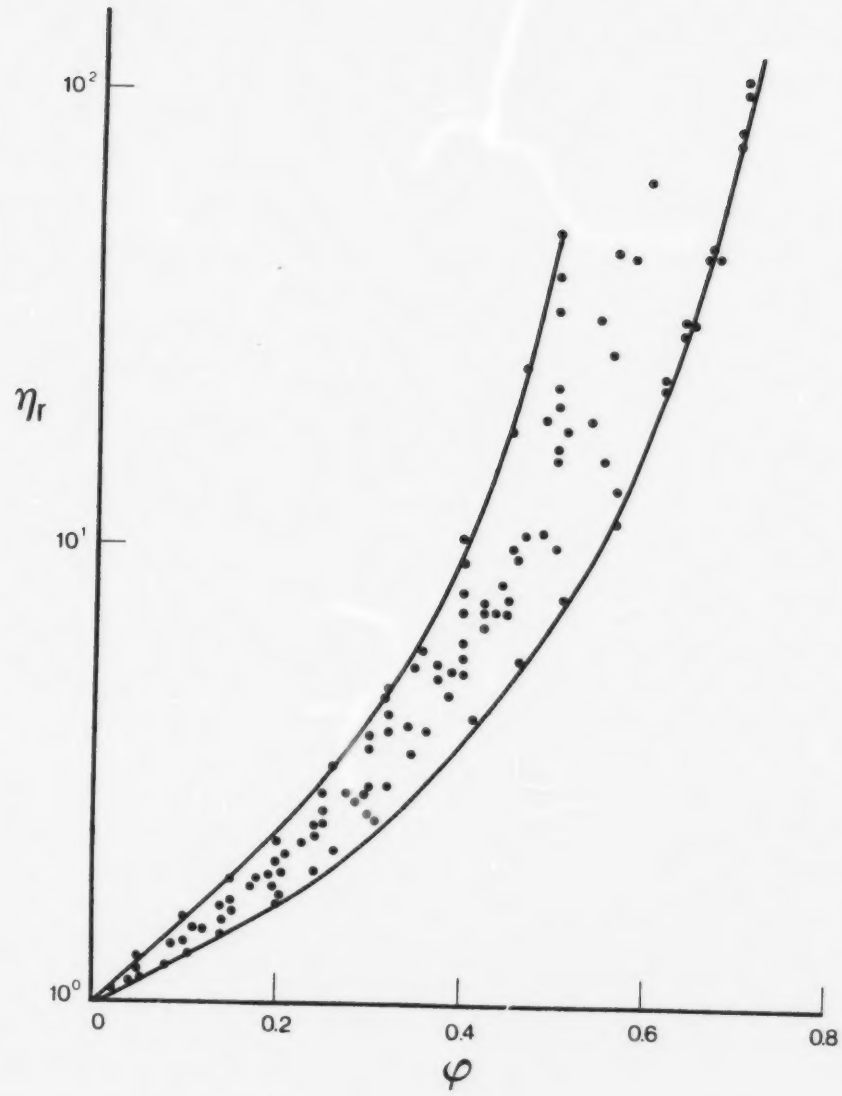
10^2
10^1
10^0
η_r
0
0.2
0.4
0.6
0.8
φ

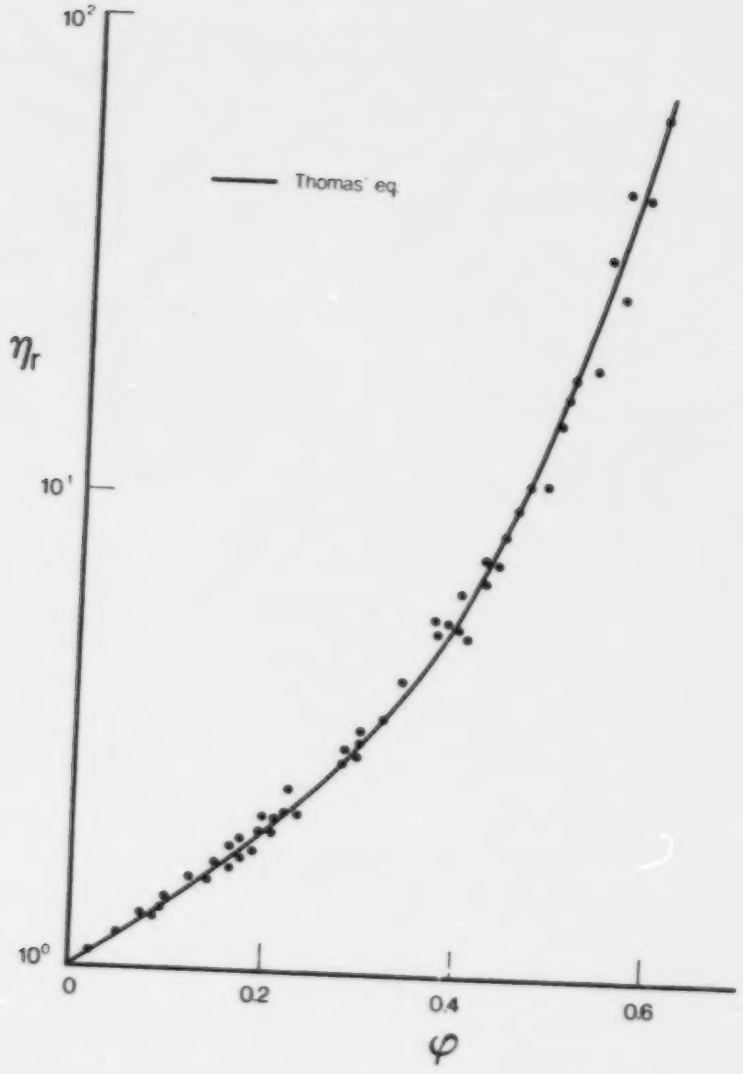
10^2
Thomas' eq.
η_r
10^1
10^0
0
0.2
0.4
0.6
φ

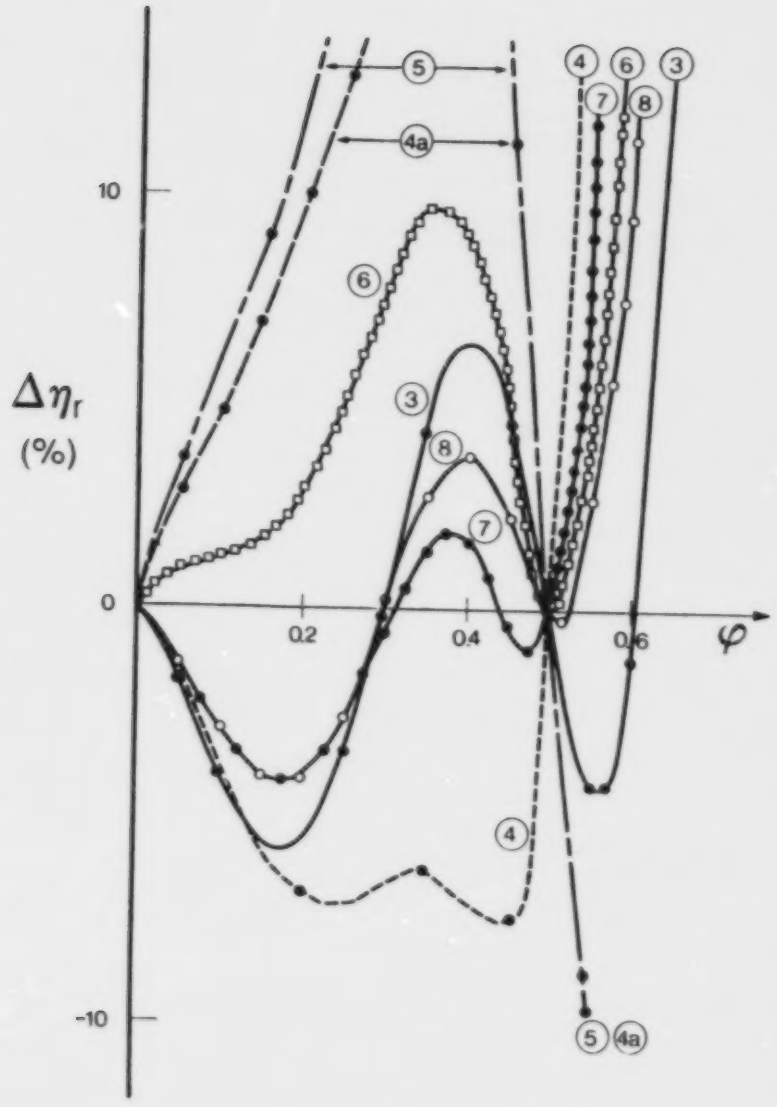
Δηr
(%)
10
0
-10
0.2
0.4
0.6
φ
5
4a
4
6
3
7
8

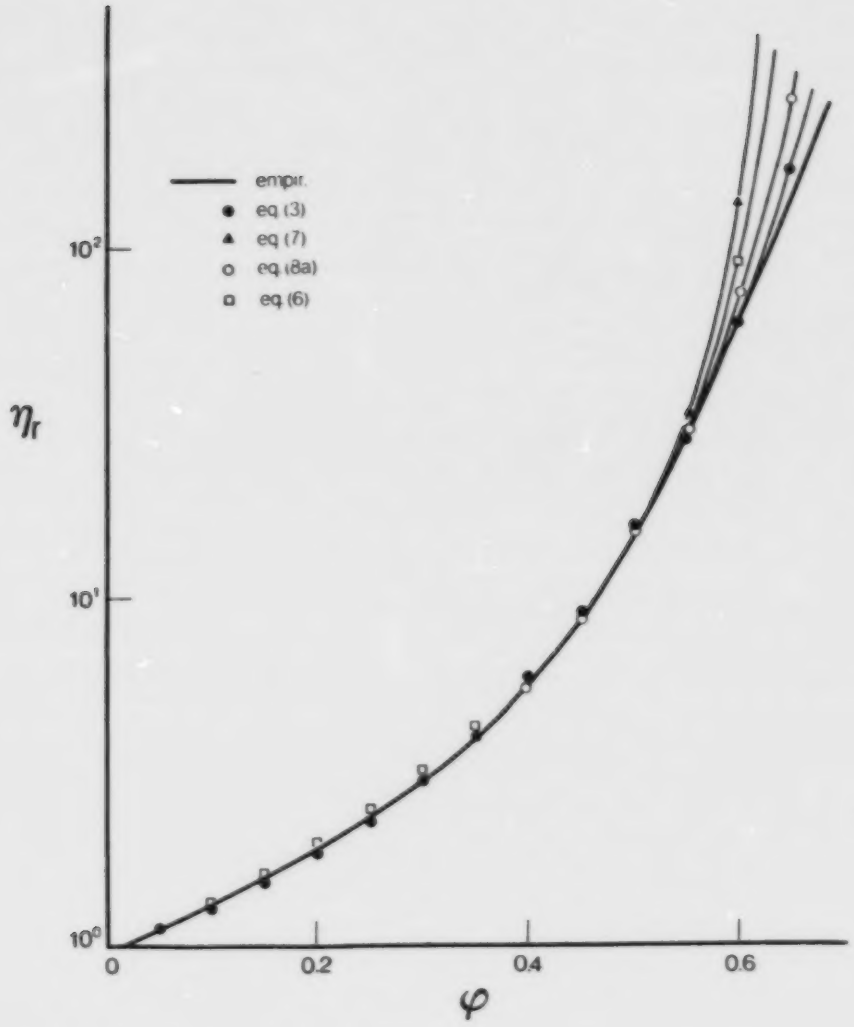
empir.
eq (3)
eq (7)
eq (8a)
eq (6)
10^2
10^1
10^0
η_r
0
0.2
0.4
0.6
φ

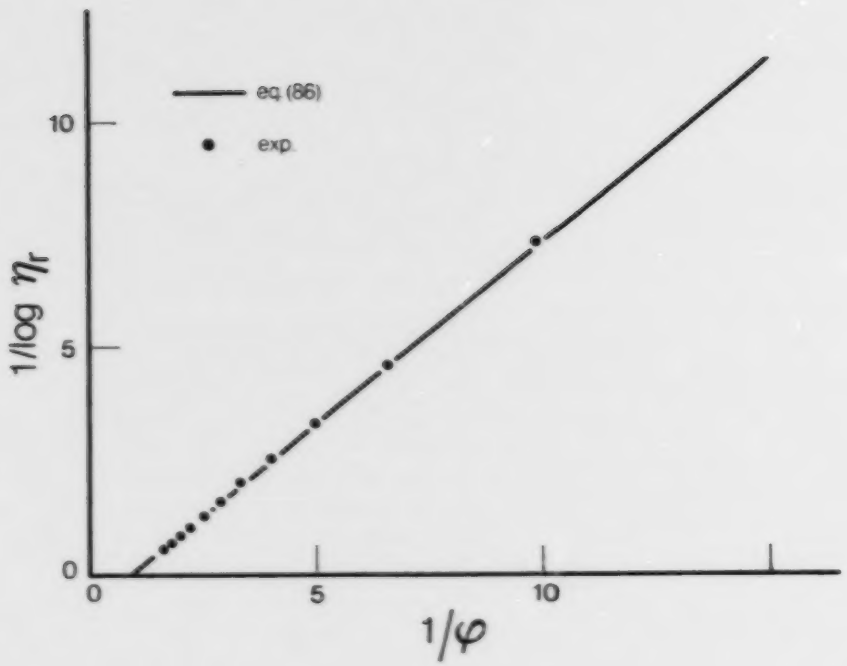
eq.(86)
exp.
10
5
0
0
5
10
1/log η_r
1/φ

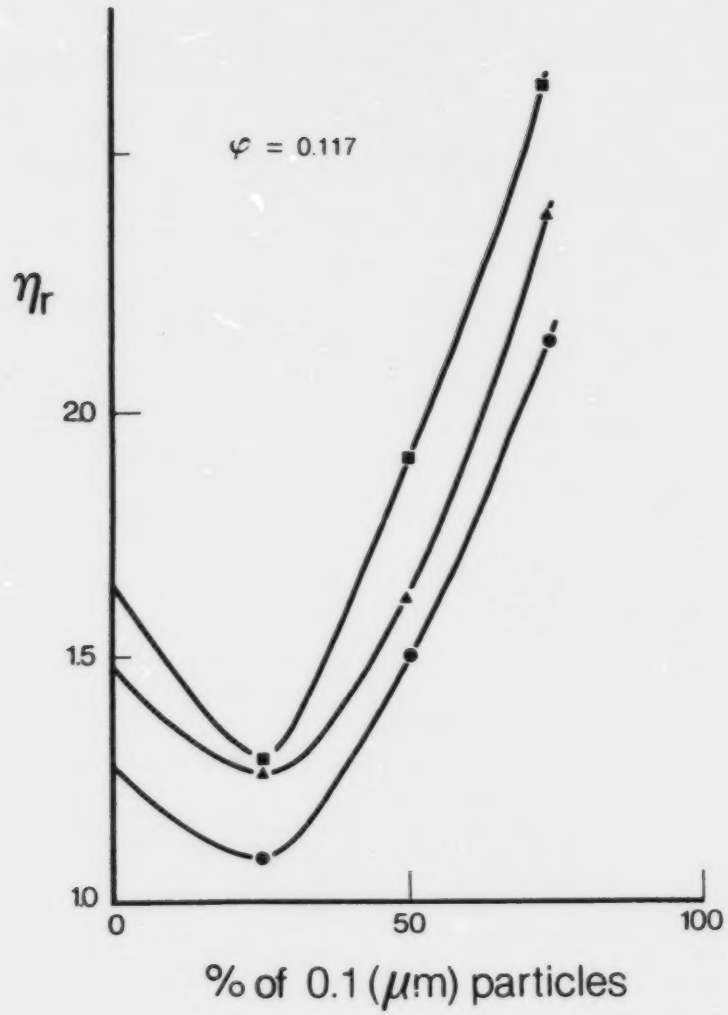
φ = 0.117
η_r
2.0
1.5
1.0
0
50
100
% of 0.1 (μm) particles

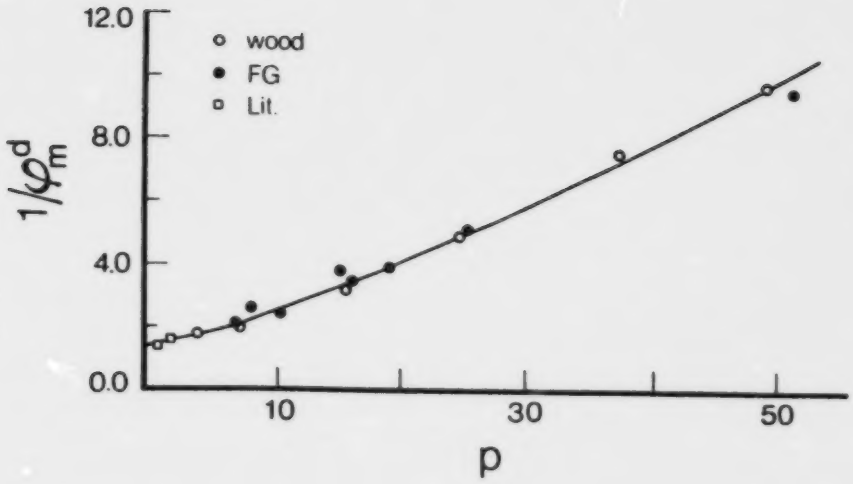
12.0
8.0
4.0
0.0
$1/\varphi_m^d$
wood
FG
Lit.
10
30
50
p

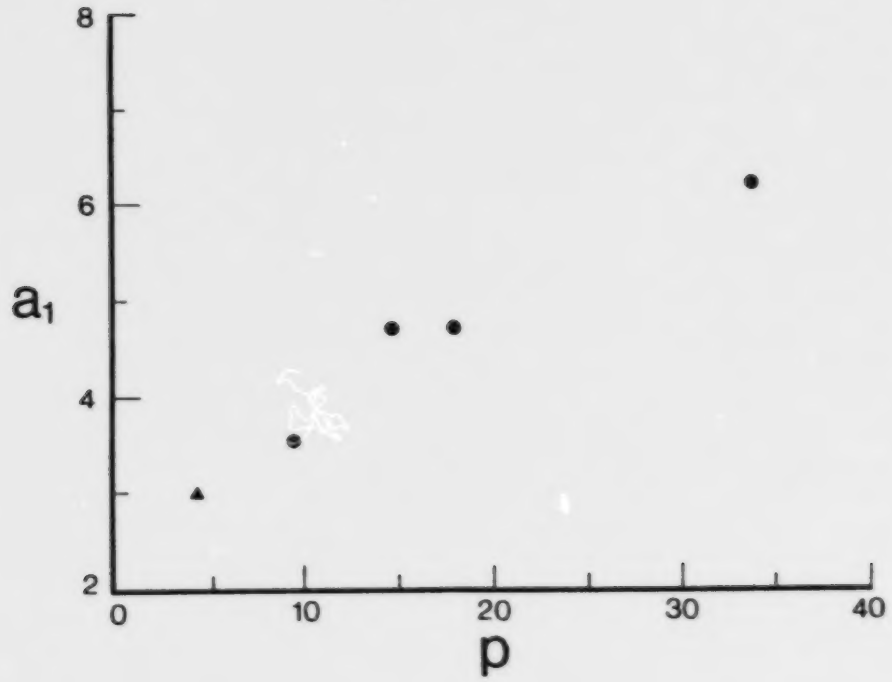
8
6
4
2
a_1
0
10
20
30
40
p

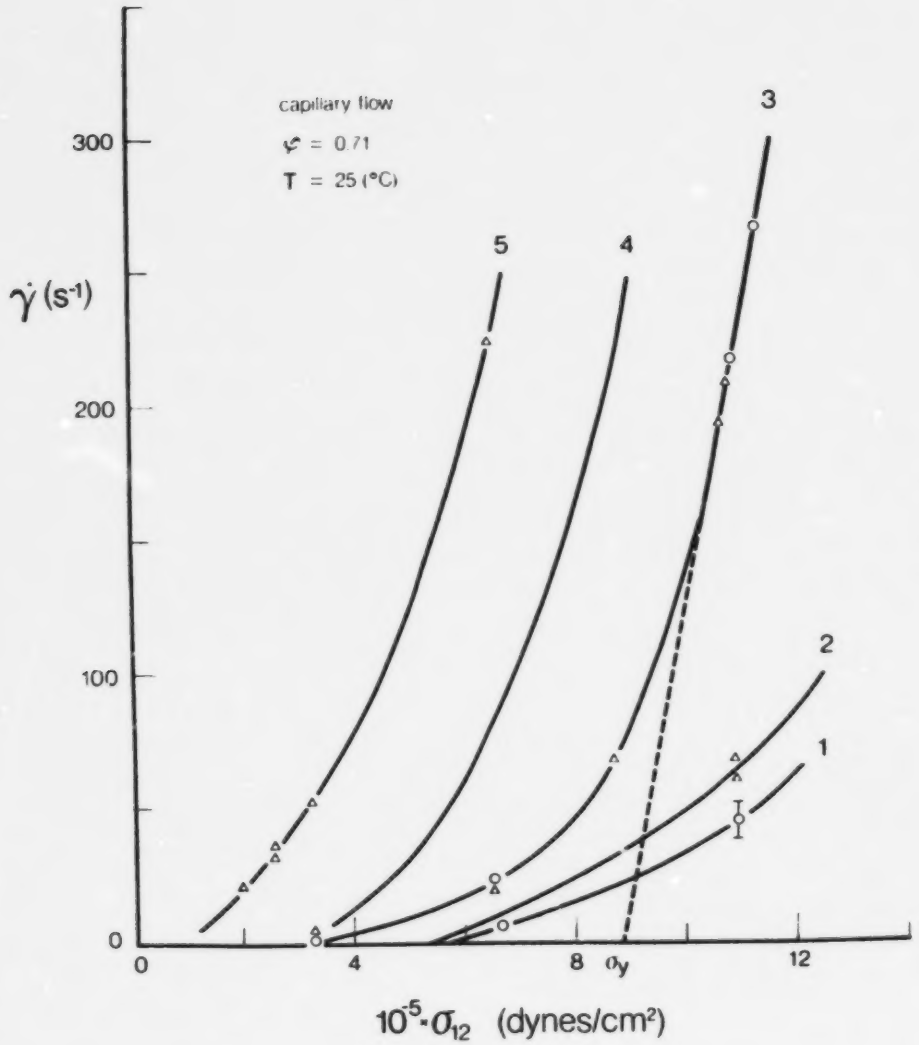
capillary flow
φ = 0.71
T = 25 (°C)
300
200
100
0
γ̇ (s⁻¹)
5
4
3
2
1
0
4
8
σy
12
10⁻⁵·σ12 (dynes/cm²)

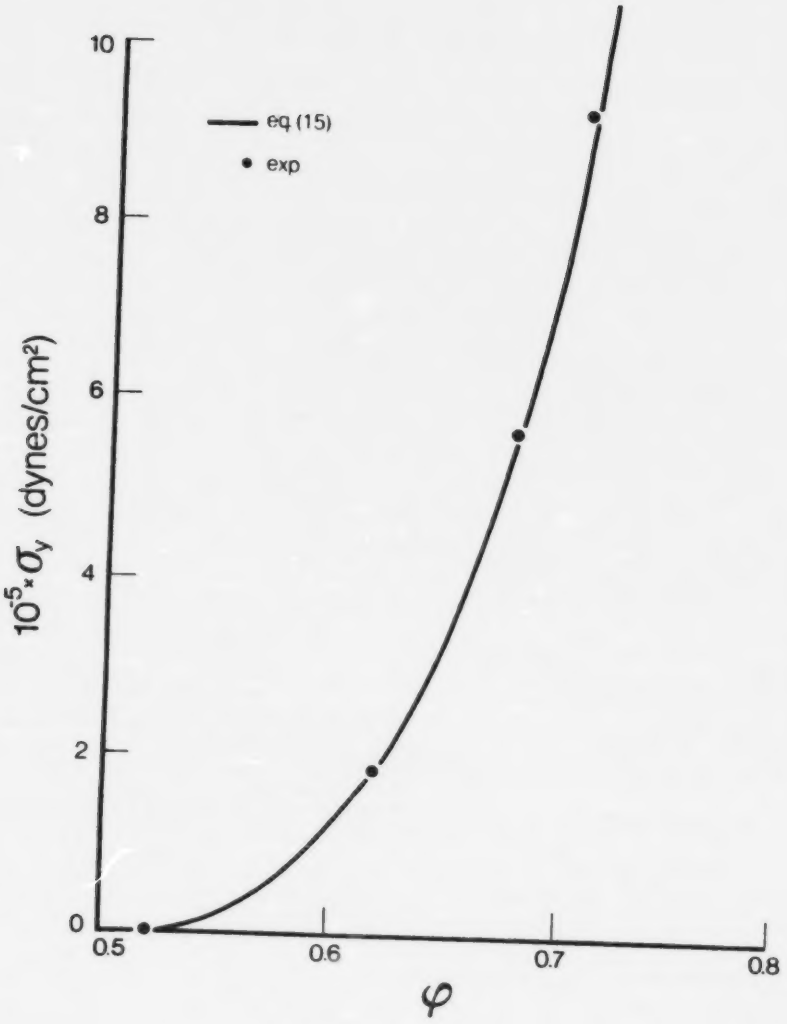
10
8
6
4
2
0
0.5
0.6
0.7
0.8
eq (15)
exp
$10^{-5} \times \sigma_y$ (dynes/cm²)
φ

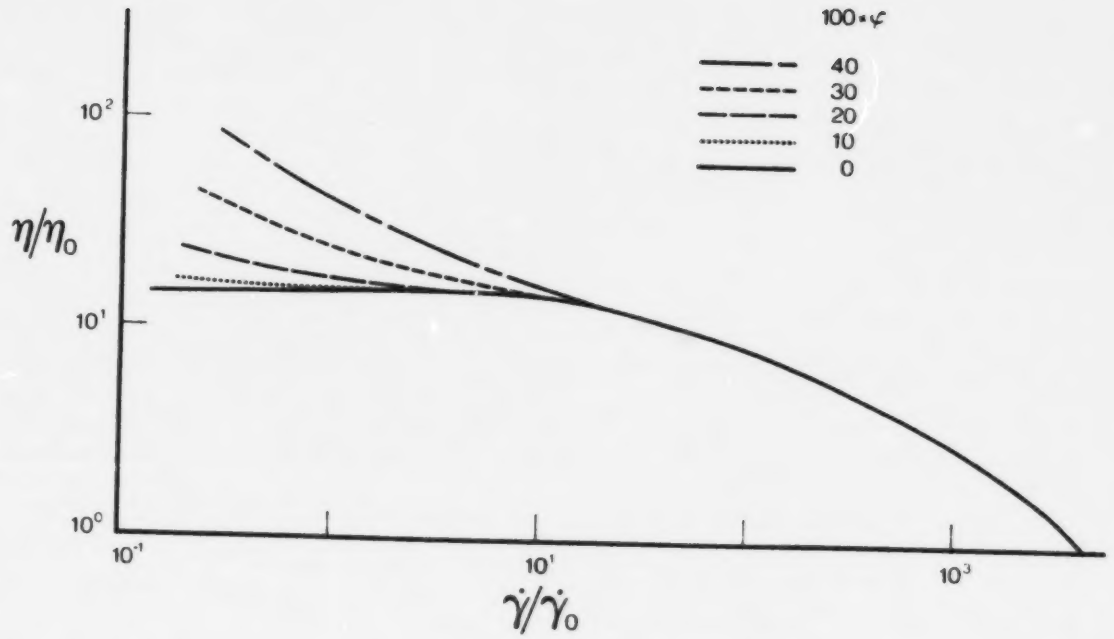
100·φ
40
30
20
10
0
10^2
10^1
10^0
η/η_0
10^{-1}
10^1
10^3
$\dot{\gamma}/\dot{\gamma}_0$

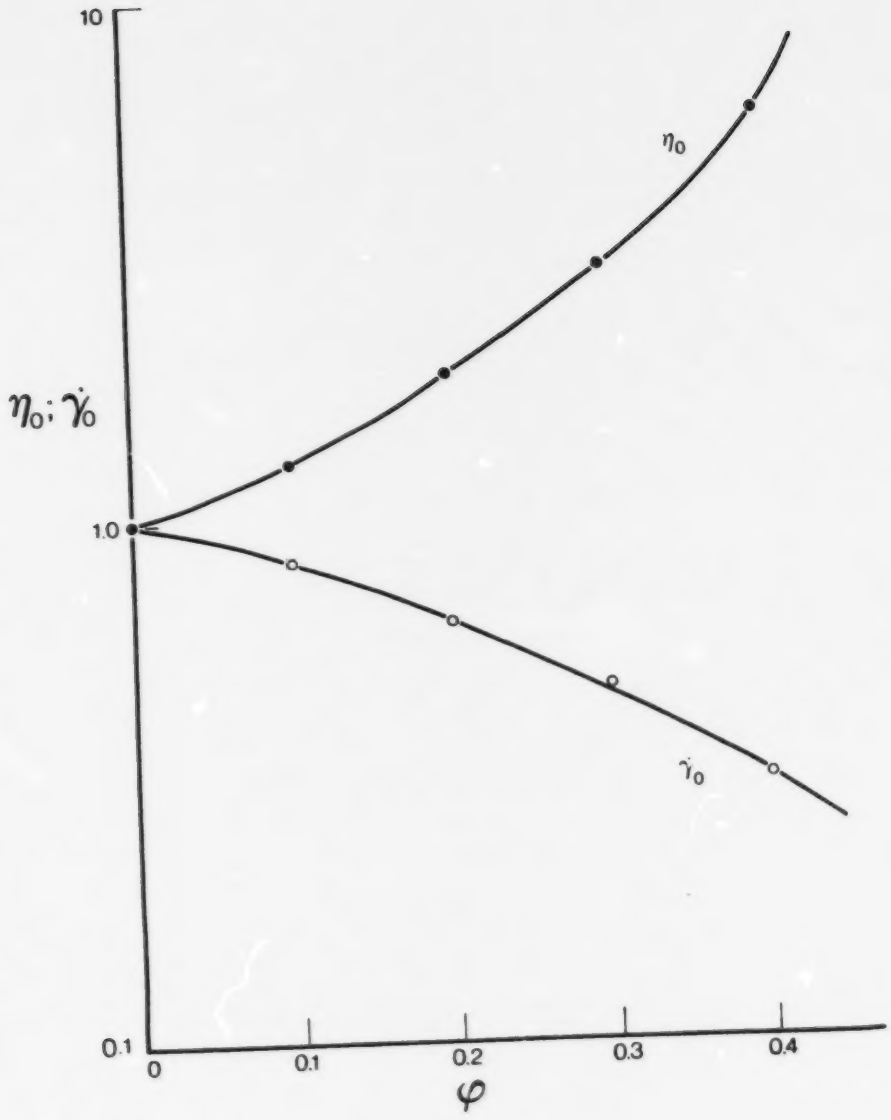
10
1.0
0.1
$\eta_0; \dot{\gamma}_0$
η_0
$\dot{\gamma}_0$
0
0.1
0.2
0.3
0.4
φ

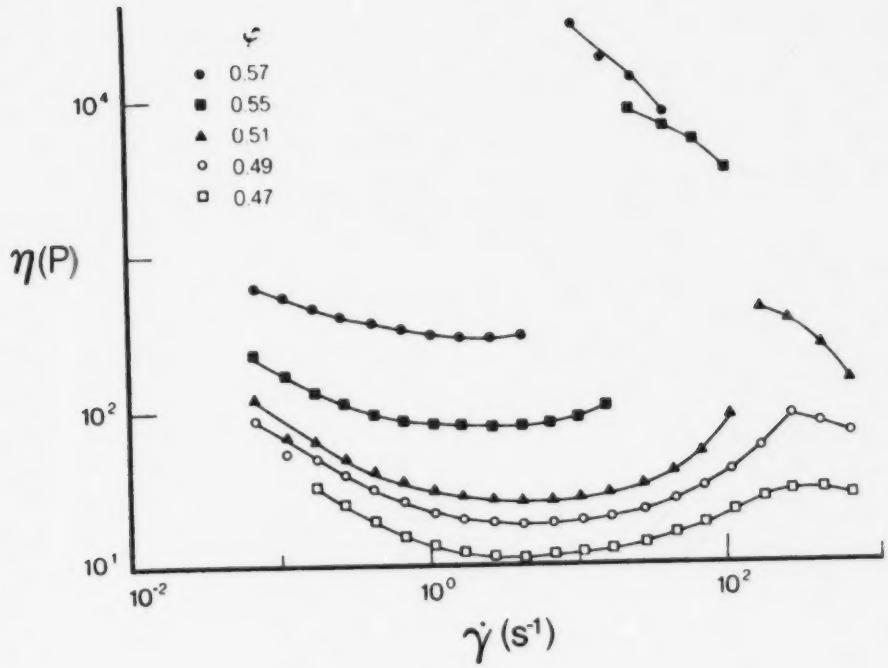
φ
0.57
0.55
0.51
0.49
0.47
10^4
10^2
10^1
η(P)
10^{-2}
10^0
10^2
$\dot{\gamma}$ (s^{-1})

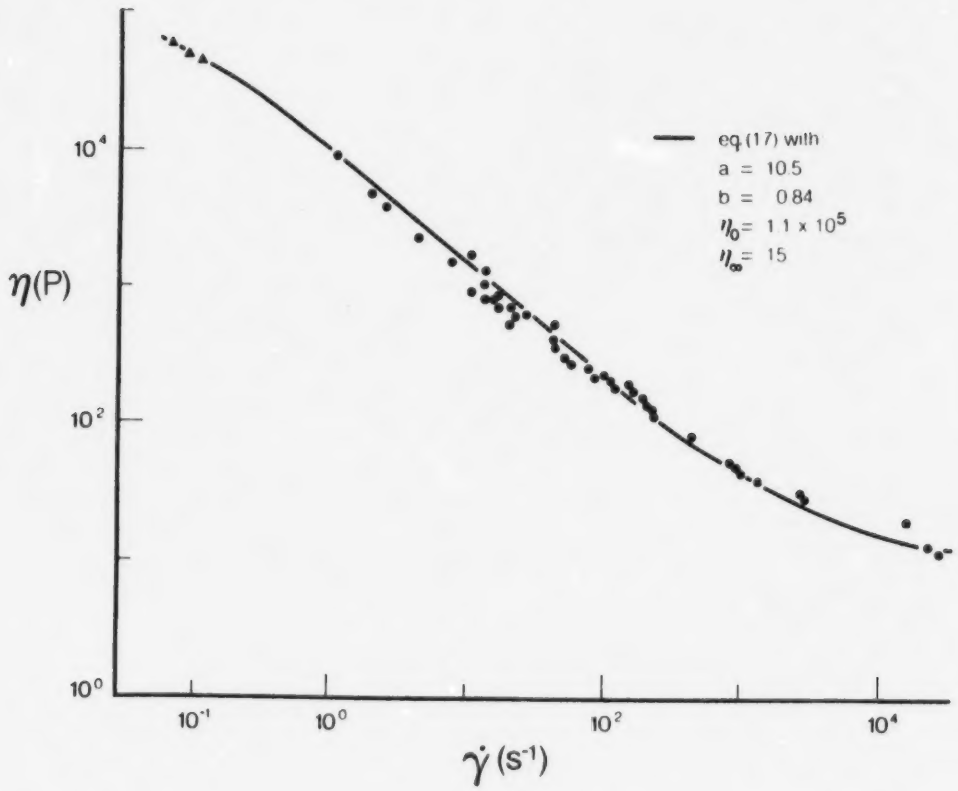
eq (17) with
a = 10.5
b = 0.84
η_0 = 1.1 x 10^5
η_∞ = 15
η(P)
10^4
10^2
10^0
10^{-1}
10^0
10^2
10^4
$\dot{\gamma}$ (s^{-1})

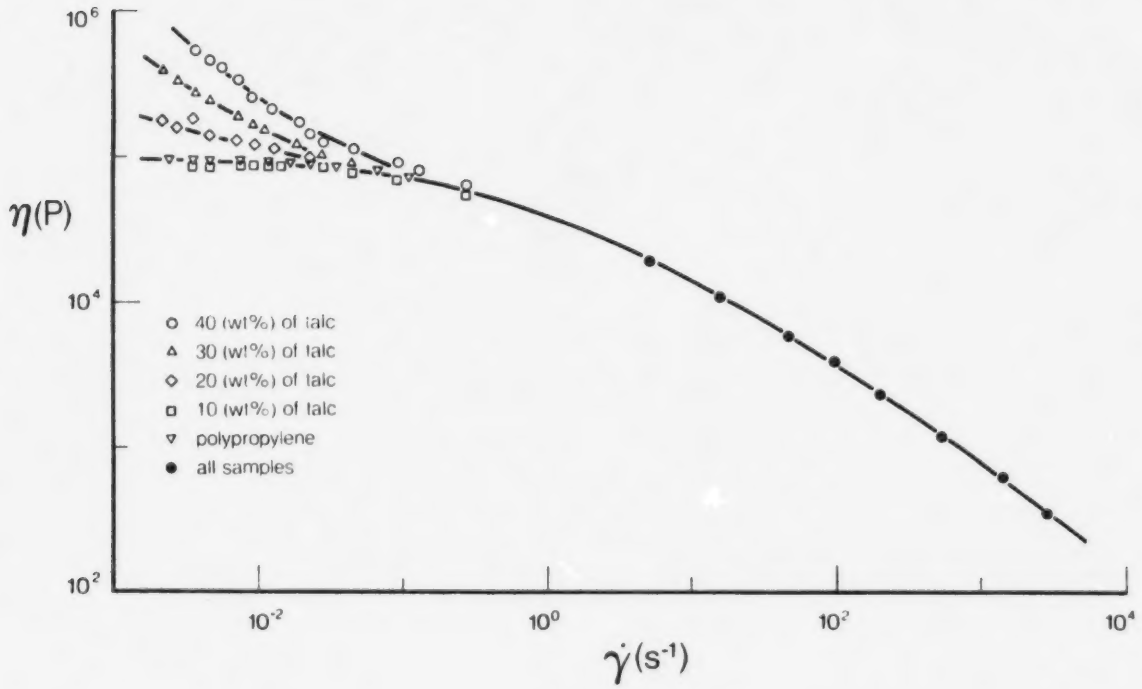
10^6
10^4
10^2
η(P)
40 (wt%) of talc
30 (wt%) of talc
20 (wt%) of talc
10 (wt%) of talc
polypropylene
all samples
10^{-2}
10^0
10^2
10^4
$\dot{\gamma}(s^{-1})$

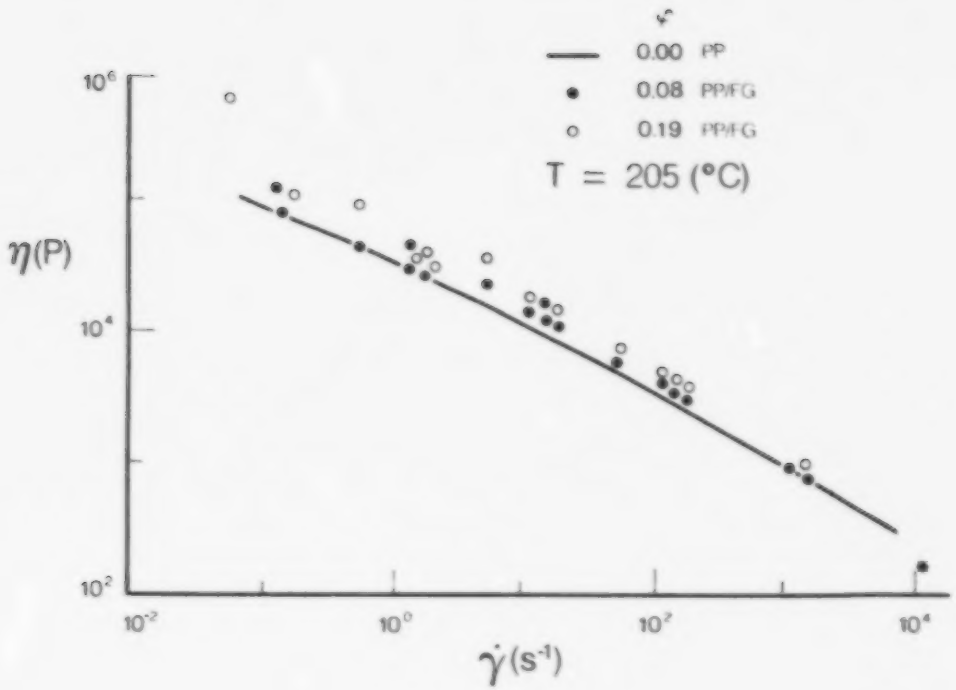
φ
0.00 PP
0.08 PP/FG
0.19 PP/FG
T = 205 (°C)
η(P)
10⁶
10⁴
10²
10⁻²
10⁰
10²
10⁴
γ̇ (s⁻¹)

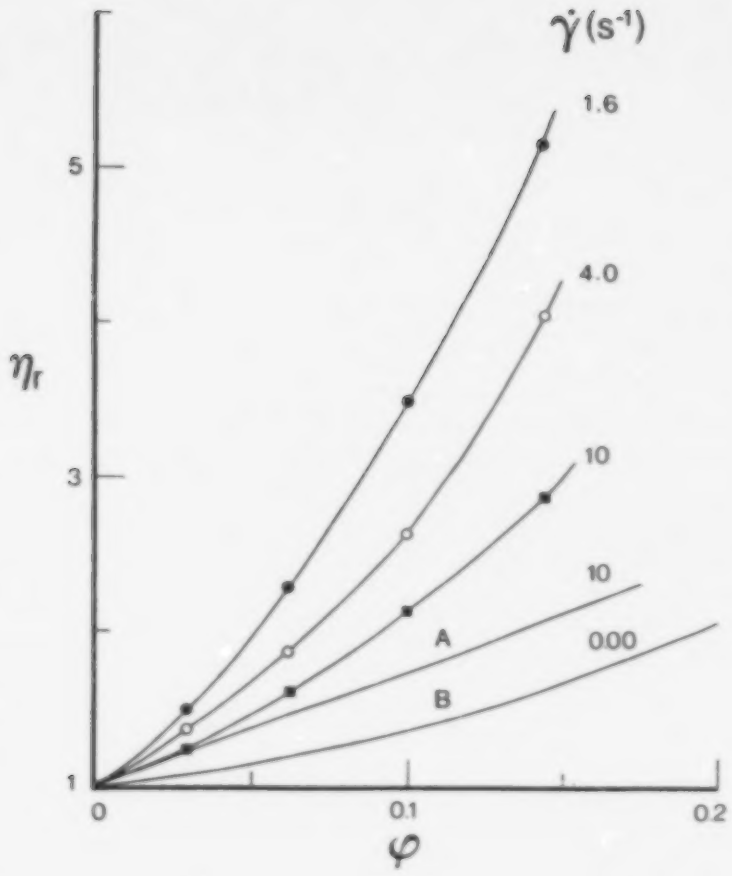
$\dot{\gamma}$ (s^{-1})
1.6
4.0
10
10
000
A
B
5
3
1
η_r
0
0.1
0.2
φ

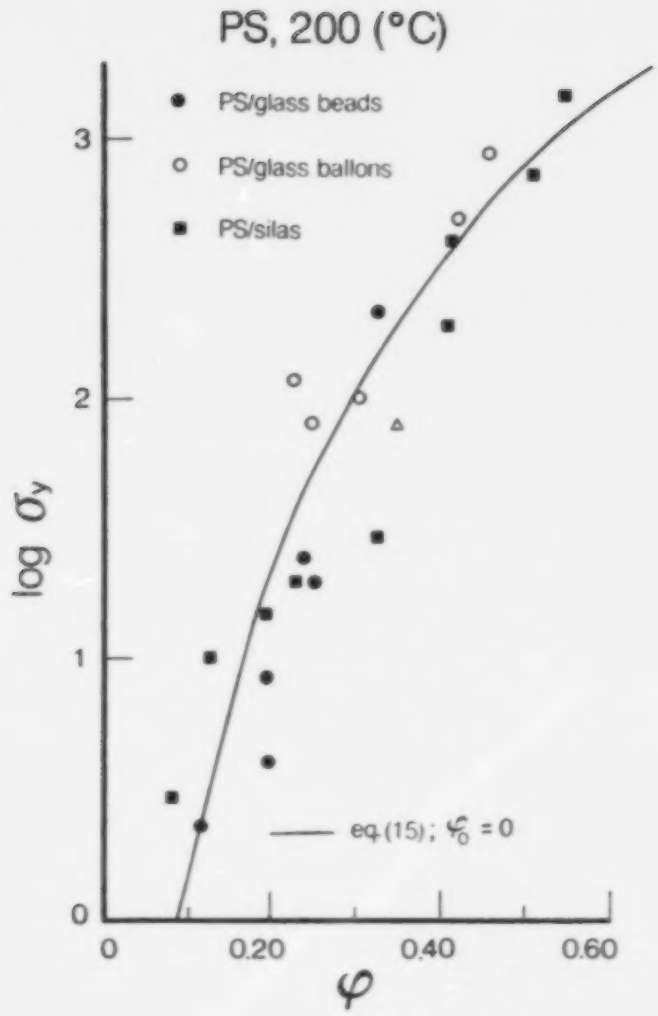
PS, 200 (°C)
PS/glass beads
PS/glass ballons
PS/silas
log σ_y
3
2
1
0
0
0.20
0.40
0.60
φ
eq.(15); $\varphi_0 = 0$

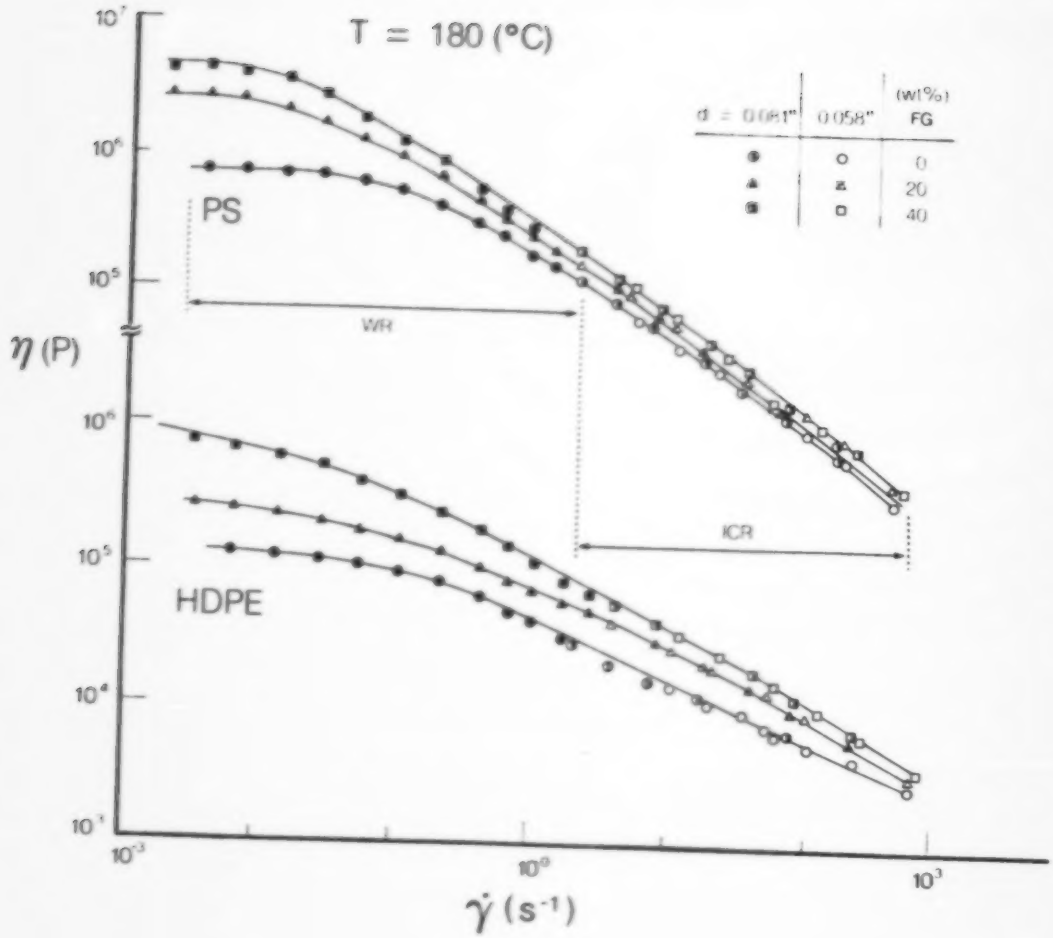
T = 180 (°C)
d = 0.081"
0.058"
(wt%) FG
0
20
40
PS
WR
ICR
HDPE
η (P)
γ̇ (s⁻¹)
10⁷
10⁶
10⁵
10⁶
10⁵
10⁴
10³
10⁻³
10⁰
10³

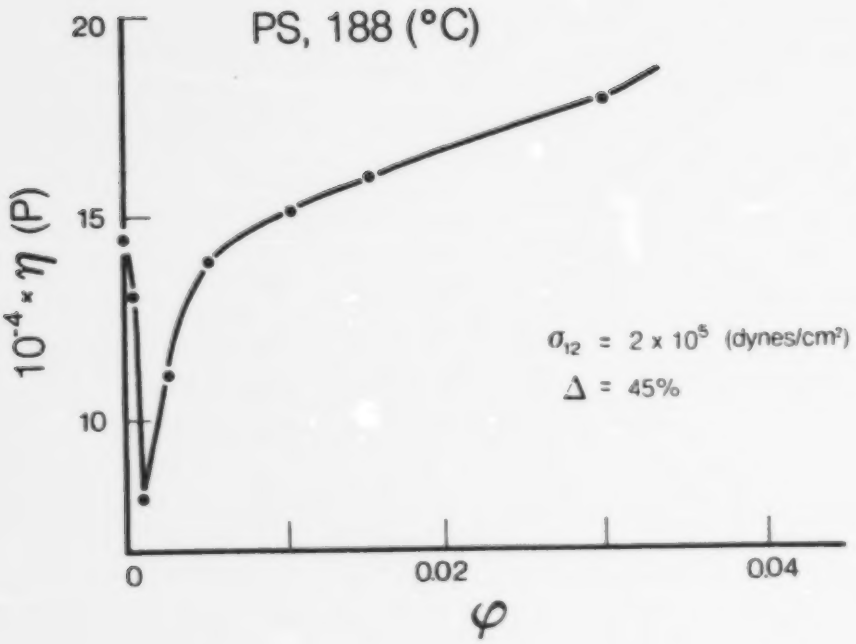
PS, 188 (°C)
20
15
10
$10^{-4} \times \eta$ (P)
σ_{12} = 2 x 10^5 (dynes/cm²)
Δ = 45%
0
0.02
0.04
φ

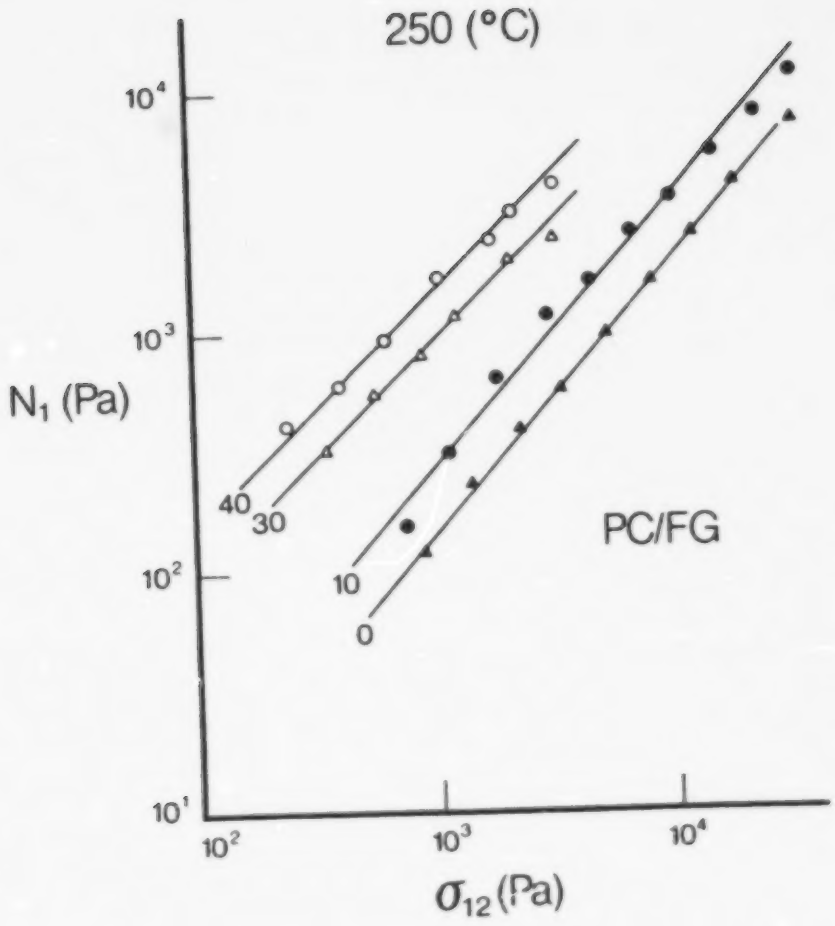
250 (°C)
10^4
10^3
10^2
10^1
N_1 (Pa)
40
30
10
0
PC/FG
10^2
10^3
10^4
σ_{12} (Pa)

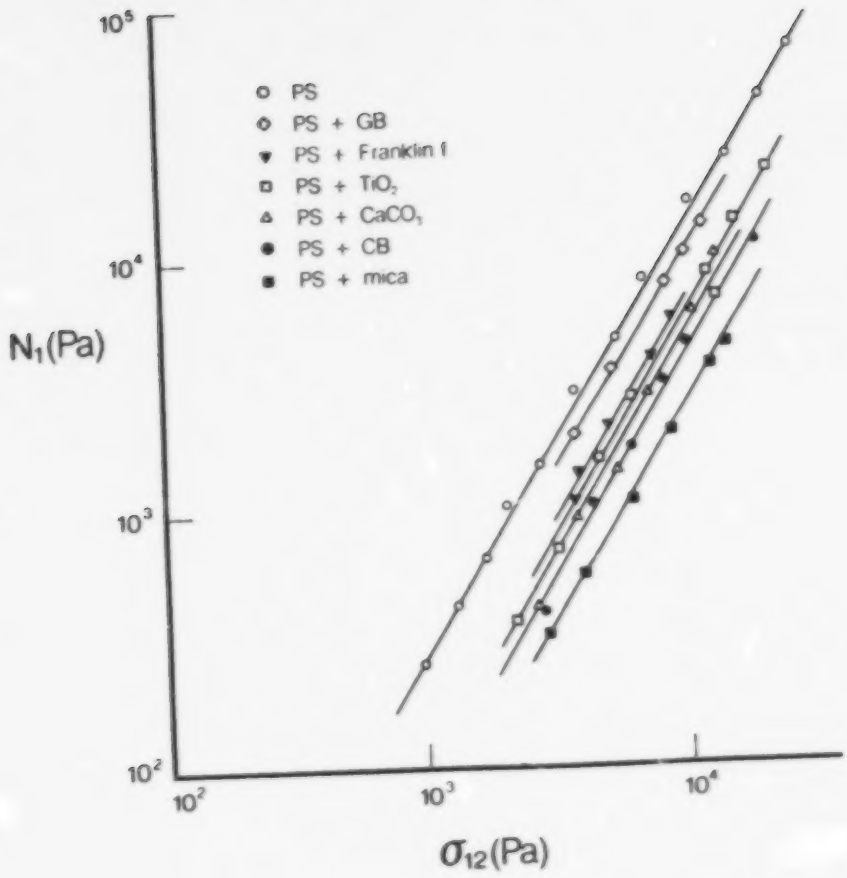
10^5
10^4
10^3
10^2
N_1(Pa)
PS
PS + GB
PS + Franklin f
PS + TiO_2
PS + $CaCO_3$
PS + CB
PS + mica
10^2
10^3
10^4
σ_{12}(Pa)

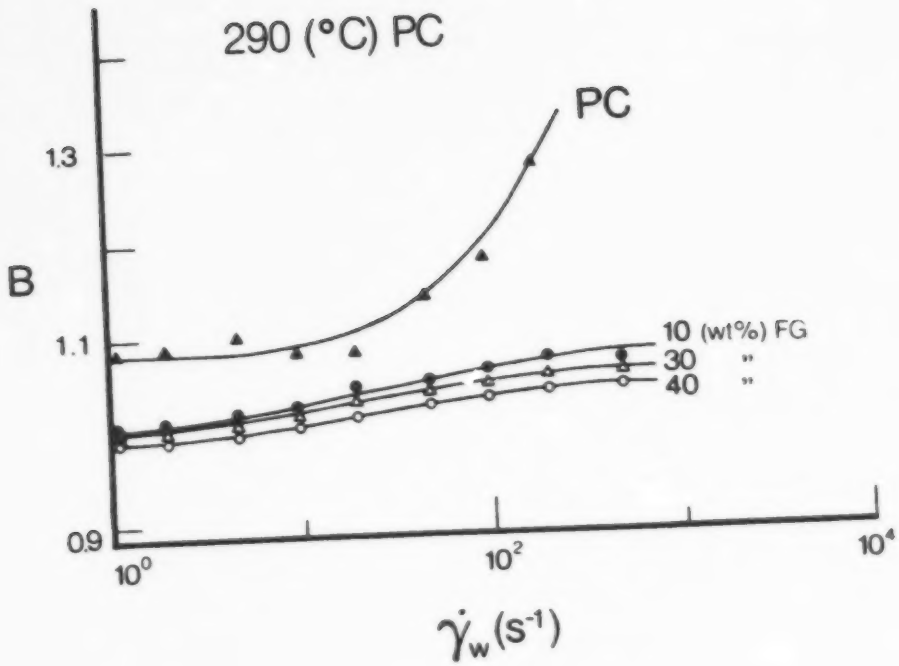
290 (°C) PC
PC
1.3
B
1.1
0.9
10 (wt%) FG
30 "
40 "
10^0
10^2
10^4
$\dot{\gamma}_w(s^{-1})$

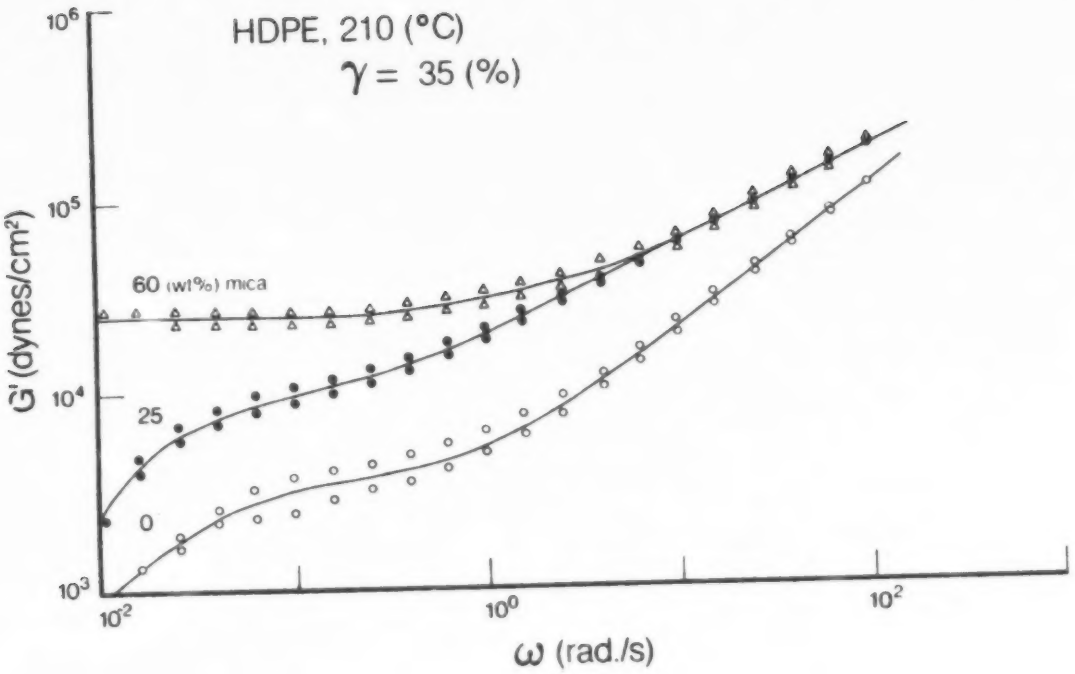
HDPE, 210 (°C)
γ = 35 (%)
10^6
10^5
10^4
10^3
G' (dynes/cm²)
60 (wt%) mica
25
0
10^-2
10^0
10^2
ω (rad./s)

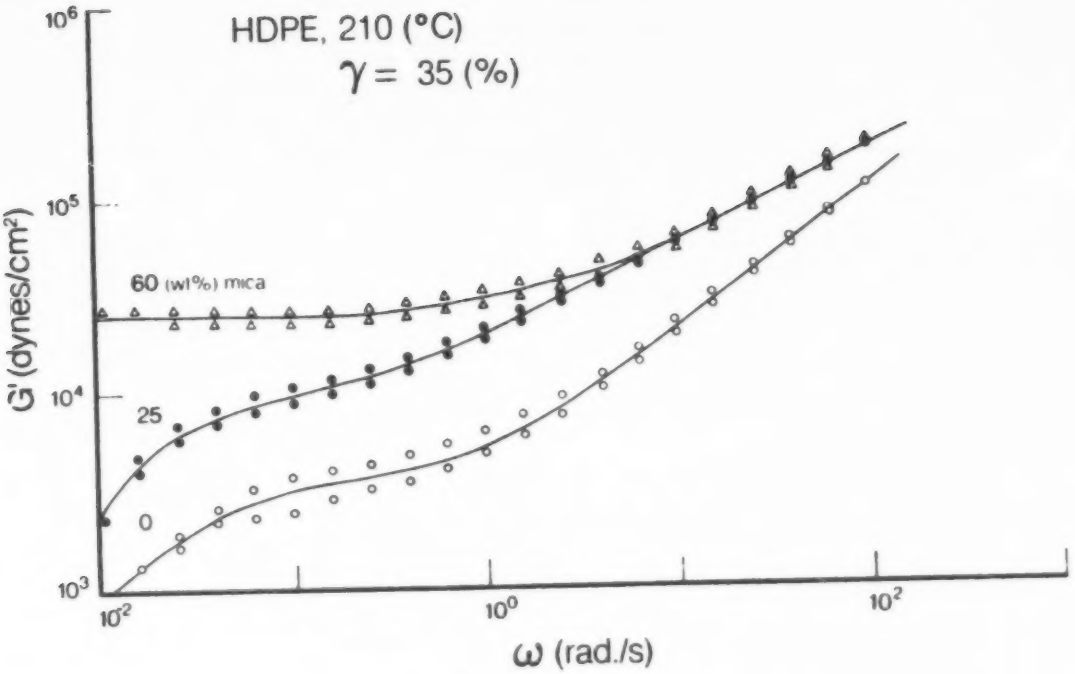
HDPE, 210 (°C)
γ = 35 (%)
10^6
10^5
10^4
10^3
G' (dynes/cm²)
60 (wt%) mica
25
0
10^-2
10^0
10^2
ω (rad./s)

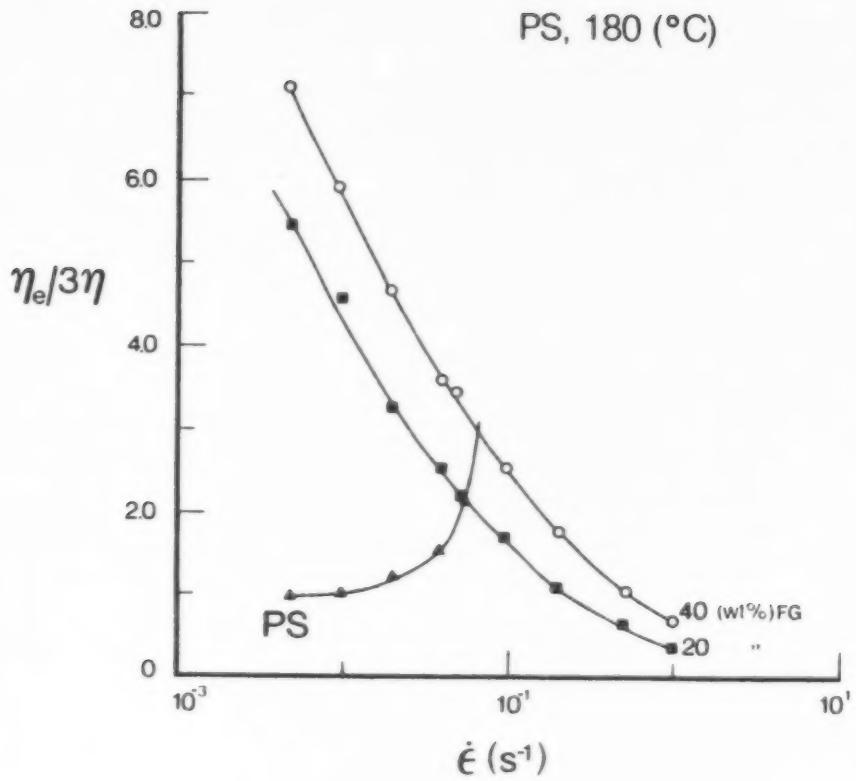
PS, 180 (°C)
8.0
6.0
4.0
2.0
0
$\eta_e/3\eta$
PS
40 (wt%)FG
20 "
10^{-3}
10^{1}
10^{1}
$\dot{\epsilon}$ (s^{-1})

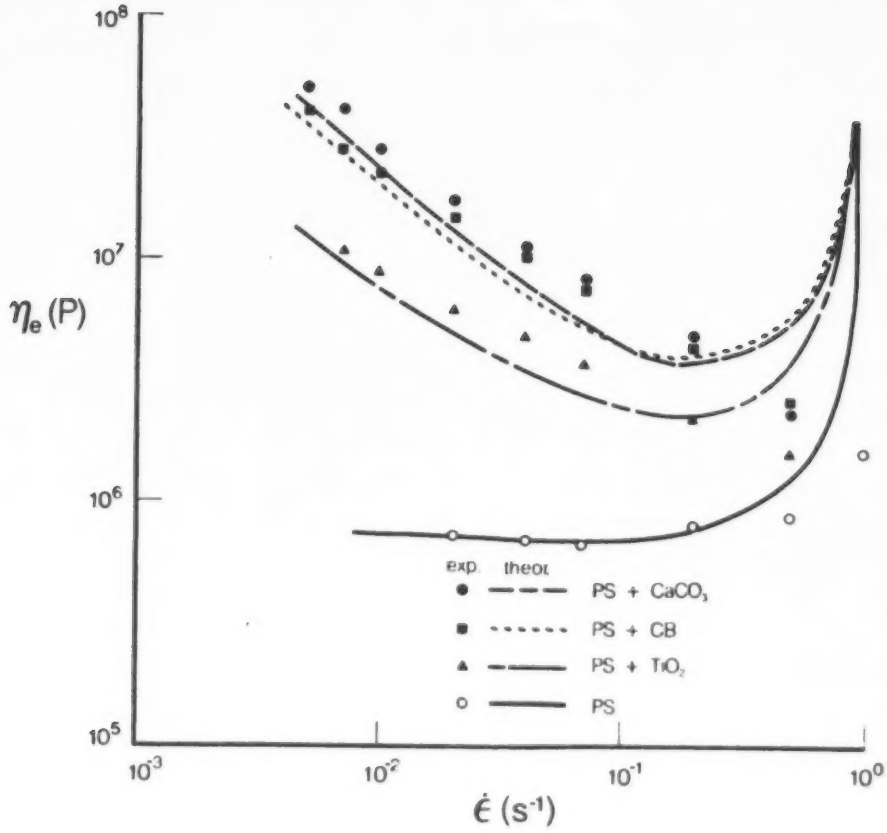
10^8
10^7
10^6
10^5
η_e (P)
exp. theor.
PS + $CaCO_3$
PS + CB
PS + TiO_2
PS
10^{-3}
10^{-2}
10^{-1}
10^0
$\dot{\epsilon}$ (s^{-1})